Chaotic advection in a cubic Stokes flow

A.I.Neishtadt[1)], D.L.Vainshtein[1,2)], and A.A.Vasiliev[1)]

[1)] Space Research Institute, Russian Academy of Science, Profsoyuznaya St. 84/32, 117810 Moscow, Russia

[2)] Department of Theoretical and Applied Mechanics, University of Illinois at Urbana-Champaign, 104 S. Wright St., Urbana, IL 61801, USA

Abstract

A stationary incompressible Stokes flow in a sphere is considered. The flow was introduced by H. A. Stone, A. Nadim and S. H. Strogatz in 1991 as a flow inside a neutrally buoyant spherical drop immersed in a linear flow. The velocity field of the flow is a result of a small perturbation of an integrable velocity field with almost all streamlines closed. Under arbitrarily small perturbation a large domain of chaotic advection within the sphere arises. This phenomenon is explained by quasi-random changes in the adiabatic invariant of the flow, which occur as a streamline crosses the two-dimensional separatrix of the unperturbed flow. Phase portraits of the averaged system are constructed. An asymptotic formula for the change in the adiabatic invariant due to the separatrix crossing is derived. The process of diffusion of the adiabatic invariant due to multiple separatrix crossings is described.

1 Introduction

Problems of chaotic advection in steady incompressible flows attract much interest in connection with impurity transport (see, for example [1]) and the fast dynamo problem [2]. In the latter context, Bajer and Moffat [3] introduced a stationary Stokes flow, confined within a sphere, possessing chaotic streamlines. In [4], another example of such a flow was represented, arising inside a spherical drop immersed in a linear steady Stokes flow. Computer simulations have shown that a considerable part of the sphere is filled

with chaotic streamlines. In both these examples the flows with chaotic streamlines are small perturbations of integrable flows, and almost all streamlines of these integrable flows are closed.

It was demonstrated in [5] that chaotic advection in the flow of [3] results from quasirandom jumps of the system's adiabatic invariant occurring each time a streamline crosses a certain surface called the separatrix of the unperturbed problem. This mechanism is remarkably revealed in a large (of order 1) size of the chaotic domain at arbitrarily small non-zero value of the perturbation.

In this paper we show that the mechanism of chaotization in the flow of [4] is similar. To describe the streamlines of the flow approximately, one can use the averaging method [7]. Averaging the motion over a fast variable, one obtains an averaged system possessing an integral. The value of this integral is conserved within an accuracy of order ε (the perturbation parameter) for time intervals of order $1/\varepsilon$ along a streamline of the exact system. This integral is called an adiabatic invariant (AI). In the vicinity of the separatrix of the unperturbed problem, however, accuracy of the averaging method decreases, because the "fast" phase changes slowly there. In this region, a detailed consideration of the AI conservation accuracy is necessary.

In the paper, we derive an asymptotic formula for the jump in the AI due to the separatrix crossing in the flow introduced in [4]. We demonstrate that the value of jump of order $\sqrt{\varepsilon}$ is much larger than the perturbation parameter, and is quasirandom: it is very sensitive to small changes in the initial conditions. Multiple separatrix crossings producing jumps in AI give rise to the diffusion of the AI by an amount of order 1 in a time $t \sim \varepsilon^{-2}$. During this time, a streamline will pass close to any point of a large region. The volume of this region is of order 1 and depends on the orientation of the perturbation vorticity vector.

There is a well-known formula for the jump in the AI due to the separatrix crossing in a one-degree-of-freedom Hamiltonian system that depends on a slowly varying parameter [8, 9, 10]. In this kind of system the separatrix of the unperturbed problem consists of trajectories passing through a family of degenerate singular points. In the present problem, as in [5], the separatrix of the unperturbed problem contains a nondegenerate singular point. Unlike in [5], the separatrix contains a family of degenerate singular points also.

We employ the method developed in [5, 6, 8, 9, 10]. In Section II we follow [4], introducing the flow under consideration and describing its properties in the absence of the perturbation. In Sec. III the perturbed flow is described with the use of the averaging method. Here we introduce the AI of the system and investigate phase portraits of the averaged system. In Section IV the dynamics in a vicinity of the separatrix is considered and the formula for the jump in the AI due to the separatrix crossing is obtained. In Section V the diffusion of the AI resulting from multiple separatrix crossings is discussed.

2 Velocity field of the flow

In this section, we mostly set forth the results obtained in [4]. Consider a spherical drop of fluid with density $\widehat{\rho}$ and viscosity $\widehat{\mu}$, suspended in a fluid with density ρ and viscosity μ. Assume that the interfacial tension is sufficiently large to maintain a spherical shape of the drop. Choose the origin of the coordinate system in the center of the drop. Far from the drop the flow is assumed to be linear: $\mathbf{u}^{\infty}(\mathbf{x}) = \mathbf{V} + \frac{1}{2}[\omega, \mathbf{x}] + E\mathbf{x}$, where $\mathbf{u}^{\infty}$ is the velocity field at infinite distance, $\mathbf{x}$ is the position vector, ω is the vorticity vector, E is the symmetric traceless rate-of-strain tensor, the square brackets here and further on denote vector product. It is possible to solve the steady incompressible Stokes flow problem and to find the velocity field inside the drop. Without loss of generality one can assume $\widehat{\mu}/\mu = 0$. In the case of $\widehat{\rho} = \rho$, $\mathbf{V} = 0$, and the drop radius equal to 1, the velocity field internal to the drop is given by

$$\mathbf{u}(\mathbf{x}) = \frac{1}{2}\left(\left(5r^2 - 3\right)E\mathbf{x} - 2\mathbf{x}\mathbf{x}^T E\mathbf{x}\right) + \frac{1}{2}[\omega, \mathbf{x}], \tag{1}$$

where $r^2 = (\mathbf{x}, \mathbf{x})$, and $\mathbf{x}^T$ is a row vector obtained by transposition of vector $\mathbf{x}$. Hence, the velocity field inside the drop is completely determined by the vorticity vector ω and tensor E, which describe the flow field far from the drop. Direct the coordinate axes along the principal axes of E so that

$$E = \pm \begin{pmatrix} E_{11} & 0 & 0 \\ 0 & E_{22} & 0 \\ 0 & 0 & -(E_{11} + E_{22}) \end{pmatrix}. \tag{2}$$

Here we have assumed that $E_{11}, E_{22} > 0$ and taken into account that $\mathrm{tr}E = 0$ (because the fluid is incompressible). No generality is lost in the kinematical discussion by focusing only on the "+" sign in (2). The external flow is directed to the origin along the z-axis, and from the origin in the (x, y)-plane, as it is shown in Fig. 1.

From now on we restrict ourselves to consideration of the axisymmetric case $E_{11} = E_{22}$. Assume also that $\omega_z \geq 0, \omega_x \geq 0, \omega_y = 0$. In spherical polar coordinates velocity field (1) takes the dimensionless form

$$\begin{aligned} \frac{dr}{dt} &= \frac{3}{4} r\left(r^2 - 1\right)\left(1 - 3\cos^2\theta\right) \\ \frac{d\theta}{dt} &= \frac{3}{4}\left(5r^2 - 3\right)\sin\theta\cos\theta - \frac{1}{2}\omega_x \sin\varphi \\ \frac{d\varphi}{dt} &= \frac{1}{2}\left(\omega_z - \omega_x \cot\theta\cos\varphi\right) \end{aligned} \tag{3}$$

The flow (3) can be considered as a superposition of two flows: a rotation at the angular velocity $\frac{1}{2}\omega$ and a flow that deforms fluid elements, defined by the terms in (3) that are independent of ω. Almost all streamlines of both flows are closed. In [4] it was demonstrated that the superposition of these flows possesses in general chaotic streamlines.

We shall treat the rotation at the angular velocity $\frac{1}{2}\omega$ as a small perturbation in (3), i.e. we put $|\omega| \ll 1$.

Consider the flow (3) in the absence of the perturbation, i.e. at $|\omega| = 0$. In this case the flow (3) turns out to be integrable. It has two independent integrals of motion: the azimuthal angle φ and the stream function

$$\psi = \frac{3}{4} r^3 \left(r^2 - 1\right) \sin^2\theta \cos\theta. \tag{4}$$

Level surfaces of integral φ are the half-planes containing the z-axis as their border. Level surfaces of integral ψ form two families of nested tori filling the northern and the southern hemispheres of the unit sphere. The intersection of a level surface of φ and a level surface of ψ is a streamline of the unperturbed flow. Almost all the streamlines of the unperturbed flow are closed curves (see Fig. 1). Besides the closed streamlines, there are also heteroclinic streamlines connecting stagnation points of the flow. The unperturbed flow has the following stagnation points (Fig. 1): two fixed saddle points in the poles of the sphere, a fixed saddle point at the origin, a family of degenerate fixed saddle points filling the equator, and two families of degenerate elliptic fixed points filling the circles $\psi = \pm\frac{3}{5^{5/2}}$. There are two heteroclinic streamlines connecting the origin to the poles of the sphere, two families of heteroclinic streamlines filling the surface of the sphere and connecting its poles to the equator, and a family of heteroclinic streamlines filling the equatorial plane $z = 0, x^2 + y^2 < 1$ and connecting the degenerate saddle points on the equator to the origin. This latter family plays a crucial role in discussion to follow. We shall call the part of equatorial plane $z = 0, x^2 + y^2 < 1$ the separatrix of the unperturbed flow.

Note that, using the integrals φ and ψ, one can write the unperturbed system can be written as

$$\dot{\mathbf{x}} = [\mathrm{grad}\varphi, \mathrm{grad}\psi]\,. \tag{5}$$

Systems of this kind are referred to as Nambu systems [11].

If the vorticity vector ω is different from zero and aligned along the z-axis, the system remains integrable. Indeed, in this case ψ is still the integral of motion, and $\varphi(t) = \varphi_0 + \omega t$. Therefore, streamlines are windings of the tori $\psi = \mathrm{const}$.

The flow becomes much more complicated if $\omega_x \neq 0$. In this case computer simulations show that, inside the sphere, there are regions that are filled with chaotic streamlines. It

will be shown in Section 4 that these regions occur because the perturbation makes a part of streamlines cross the separatrix of unperturbed flow, producing quasirandom changes in the adiabatic invariant of the system. On the other hand, near the circles $\psi = \pm\frac{3}{5^{5/2}}$ at small enough $|\omega|$ and $\frac{\omega_z}{\omega_x} > \frac{1}{\sqrt{2}}$ there exist regions of regular dynamics. These regions are filled, up to a residual of small measure, with streamlines that do not cross the separatrix. The size of these regions was estimated in [4] based on the averaging of the equations of motion (3) in a small vicinity of these circles.

3 The averaging method and phase portraits of the averaged system

If the vorticity vector ω has non-zero component ω_x, streamlines of the flow (3) are not closed; some of them cross the separatrix of the unperturbed flow (see Fig. 2a and 2b, where two projections of a segment of a perturbed streamline crossing the separatrix are shown).

At small non-zero values of ω_z and ω_x, the flow (3) can be approximately described based on an averaging method. A point inside the sphere that does not lie on the z-axis can be specified by the coordinates ψ, φ, s, where ψ, φ are the values of the unperturbed system integrals, and $s\,(\mathrm{mod}2\pi)$ is the phase (angle variable) along the unperturbed streamline passing through the point under consideration. In terms of the new variables the perturbed system has the following form:

$$\begin{aligned} \dot{\psi} &= \varepsilon f(\psi, \varphi, s), \\ \dot{\varphi} &= \varepsilon g(\psi, \varphi, s), \\ \dot{s} &= \Omega(\psi, \varphi) + \varepsilon h(\psi, \varphi, s), \end{aligned} \tag{6}$$

where $\varepsilon = |\omega|$, and functions f, g, h are 2π-periodic in s. Define the averaged system:

$$\begin{aligned} \dot{\psi} &= \varepsilon F(\psi, \varphi), \\ \dot{\varphi} &= \varepsilon G(\psi, \varphi), \end{aligned} \tag{7}$$

where functions F and G are the averages of f and g over one period of s. It follows from this definition that

$$
\begin{aligned}
F(\psi,\varphi) &= \frac{1}{T(\psi,\varphi)}\oint(\mathrm{grad}\psi,\mathbf{v})\,dt,\\
G(\psi,\varphi) &= \frac{1}{T(\psi,\varphi)}\oint(\mathrm{grad}\varphi,\mathbf{v})\,dt,
\end{aligned}
\tag{8}
$$

where $\mathbf{v}=\frac{1}{2}\frac{[\omega,\mathbf{x}]}{|\omega|}$ is the perturbation vector field, the integrals are evaluated along a streamline of the unperturbed system $\Gamma_{\psi,\varphi}$ defined by the values of ψ and φ, and $T(\psi,\varphi)$ is the period of the unperturbed motion along this streamline. Far from the separatrix, the solutions of the averaged system describe the behavior of ψ and φ along a streamline of the exact system (3) to an accuracy of order ε over time intervals of order $1/\varepsilon$ [7, 12].

Denote by $\Phi(\psi,\varphi)$ the flux of the perturbation vector $\mathbf{v}$ across a surface S spanning the streamline of the unperturbed system $\Gamma_{\psi,\varphi}$. This flux depends on ψ and φ and is independent of the choice of the spanning surface, since the flow is incompressible. Thus

$$
\Phi(\psi,\varphi)=\int_S(\mathbf{v},\mathbf{n})\,d\sigma, \tag{9}
$$

where $\mathbf{n}$ and $d\sigma$ are the unit normal on S and an area element on S. The positive direction of $\mathbf{n}$ is defined as follows. On the surface S, there is the natural direction of rotation, specified by the unperturbed motion along its edge. The positive direction of the normal is taken to be the direction of the angular velocity of this rotation. The following formulas are derived in Appendix, establishing a connection between $\Phi(\psi,\varphi)$ and the r.h.s. of the averaged system (see also [5]):

$$
\begin{aligned}
F(\psi,\varphi) &= -\frac{1}{T(\psi,\varphi)}\frac{\partial\Phi(\psi,\varphi)}{\partial\varphi},\\
G(\psi,\varphi) &= \frac{1}{T(\psi,\varphi)}\frac{\partial\Phi(\psi,\varphi)}{\partial\psi}.
\end{aligned}
\tag{10}
$$

Thus, the averaged system is a Hamiltonian system with the volume form $T(\psi,\varphi)\,d\psi\wedge d\varphi$ and the Hamiltonian function $\Phi(\psi,\varphi)$. In particular, it follows that $\Phi(\psi,\varphi)$ is an integral of the averaged system. On the separatrix the averaged system is not defined and the function Φ is discontinuous. Below, we redefine Φ so that it is continuous.

We next derive an asymptotic expansion for $\Phi(\psi,\varphi)$ near the separatrix, i.e. at $|\psi|\ll 1$. At small values of $|\psi|$ and fixed φ, the unperturbed streamline $\Gamma_{\psi,\varphi}$ is close to the limit contour $\Gamma_{0,\varphi}$, consisting of two radii of the sphere (one connecting the center of

the sphere to its pole, and the other belonging to the equatorial plane) and the arc on the surface of the sphere connecting the pole with the point on the equator. To evaluate $\Phi(\psi,\varphi)$, we use the following formula equivalent to (9):

$$\Phi(\psi,\varphi)=\oint_{\Gamma_{\psi,\varphi}}(\mathbf{A},d\mathbf{l}), \tag{11}$$

where $\mathbf{A}$ is a vector potential of the perturbation $\mathbf{v}$: $\mathrm{rot}\mathbf{A}=\mathbf{v}$, and $d\mathbf{l}$ is the length element on the contour $\Gamma_{\psi,\varphi}$. The direction of the integration is the direction of the unperturbed motion along $\Gamma_{\psi,\varphi}$. Renormalize the vector ω: $\omega_x\to\varepsilon\omega_x,\omega_z\to\varepsilon\omega_z$, so that $|\omega|=1$, and choose the vector potential of the perturbation in the form

$$\mathbf{A}=(A_r,A_\theta,A_\varphi)=\left(\frac{r^2}{2}(\omega_z\cos\theta+\omega_x\sin\theta\cos\varphi),0,\frac{1}{r\sin\theta}\right). \tag{12}$$

Along the unperturbed streamline $d\varphi=0$. Taking into account closeness between the contours $\Gamma_{\psi,\varphi}$ and $\Gamma_{0,\varphi}$ at $|\psi|\ll 1$, we find:

$$\begin{aligned}\Phi(\psi,\varphi) &= \oint_{\Gamma_{\psi,\varphi}}A_r dr=\frac{1}{2}\omega_z\oint_{\Gamma_{\psi,\varphi}}r^2\cos\theta dr+\frac{1}{2}\omega_x\cos\varphi\oint_{\Gamma_{\psi,\varphi}}r^2\sin\theta dr\\ &= -\left(\frac{1}{6}\omega_z\mathrm{sign}(\psi)+\frac{1}{6}\omega_x\cos\varphi-2a(\varphi)\omega_x\sqrt{|\psi|}+O(\psi\ln|\psi|)\right),\end{aligned} \tag{13}$$

where

$$a(\varphi)=\frac{1}{2\sqrt{3}}\cos\varphi\int_0^1\sqrt{\frac{r}{1-r^2}}dr=\frac{1}{\sqrt{6\pi}}\Gamma^2\left(\frac{3}{4}\right)\cos\varphi. \tag{14}$$

Here $\Gamma(.)$ denotes the Γ-function. The first two terms in (13) give the circulation of $\mathbf{A}$ along $\Gamma_{0,\varphi}$. The third term is singular in ψ and is the leading term in the asymptotic expansion of $\Phi(\psi,\varphi)$ at small ψ. In order to avoid a break in Φ on the separatrix, we redefine $\Phi(\psi,\varphi)$ as follows: $\widetilde{\Phi}=\Phi+\frac{\omega_z}{6}\mathrm{sign}(\psi)$. From now on, the tilda is omitted.

Consider phase portraits of the averaged system. In [4] the portraits were based on an approximate description of the averaged system in a small vicinity of degenerate elliptic points of (3), i.e. at $\psi\approx\pm\frac{3}{5^{5/2}}$. As was noted in [4], these portraits can not describe correctly the behavior of the averaged system near the separatrix. The phase space of the averaged system is a cylinder $\left[-\frac{3}{5^{5/2}};\frac{3}{5^{5/2}}\right]\times S^1$. We introduce parameter $\beta=\frac{\omega_z}{\omega_x}$. At $\omega_x=0$ (i.e. at an infinitely large value of β), phase curves of the averaged system are the circles $\psi=\mathrm{const},\varphi(t)=\varphi_0+\omega_z t$.

Computer simulations of the system (3) show that for β in the range $\infty > \beta > 1/\sqrt{2}$ there are two pairs of stationary points (stable and unstable in each pair) at $\varphi = 0, \pi$. It follows from (13) that the stable points lie on the separatrix (i.e. at $\psi = 0$). Hence, at $\beta > 1/\sqrt{2}$ the phase portrait looks like that shown in Fig. 3a. Singularity of the integral curves $\Phi = \text{const}$ on the separatrix (at $\psi = 0$) can be found from formula (13). Let an integral curve cross the separatrix at $\varphi = \varphi_0$. Then at $\varphi = \varphi_0 + \delta\varphi$, where $|\delta\varphi| \ll 1$, this integral curve is defined by

$$\sqrt{|\psi|} = -\frac{\sqrt{\pi}\tan\varphi_0}{2\sqrt{6}\Gamma^2(3/4)}\delta\varphi. \tag{15}$$

From (15), one can see that the integral curve is defined for $\delta\varphi > 0$, if $\varphi_0 \in \left(\frac{\pi}{2}, \pi\right) \cup \left(\frac{3\pi}{2}, 2\pi\right)$, and $\delta\varphi < 0$, if $\varphi_0 \in \left(0, \frac{\pi}{2}\right) \cup \left(\pi, \frac{3\pi}{2}\right)$. If $\varphi_0 = \frac{\pi}{2}, \frac{3\pi}{2}$, the integral curve is defined in a small vicinity of φ_0 both for positive and negative values of $\delta\varphi$. This integral curve is given by the equation $\Phi(\psi, \varphi) = 0$. It is essential that a phase point moving along an integral curve approach the separatrix and leave it in a finite time. In Fig. 3a one can see that for $\beta > \frac{1}{\sqrt{2}}$, there are three kinds of phase trajectories of the averaged system: trajectories not crossing the separatrix; trajectories crossing the separatrix and enclosing the phase cylinder; and trajectories crossing the separatrix and encircling stable points of the phase portrait.

On the phase portrait of the averaged system, there are regions filled with phase trajectories that do not cross the separatrix. These regions correspond to the regions of regular streamlines of the flow (3), surrounding the circles $\psi = \pm\frac{3}{5^{5/2}}$. It is shown in [4] that the size of these regions depends on the parameter β, and as β approaches $\beta_{crit} = \frac{1}{\sqrt{2}}$ these regions shrink to zero. On the phase portrait of the averaged system, it means that the unstable stationary points at $\varphi = 0, \pi$ approach the phase cylinder borders $\psi = \pm\frac{3}{5^{5/2}}$. The phase portrait at $\beta = \beta_{crit}$ is shown in Fig. 3b. Finally, for $\beta < \frac{1}{\sqrt{2}}$ each of these stationary points splits into two saddles (see Fig. 3c), and all the phase trajectories cross the separatrix.

Far from the separatrix, the AI function Φ is conserved along the streamlines of system (3) to accuracy of order ε on time intervals of order $1/\varepsilon$. The behavior of the AI near the separatrix is considered in the next section.

4 Change in the adiabatic invariant due to the separatrix crossing

Under the perturbation considered in Section 2, values of ψ and φ change along a streamline at a rate of order ε. As a result, the streamline is not a closed curve as in the absence of the perturbation, but a spiral which may cross the separatrix, passing from one hemisphere to the other. Consider a segment of a perturbed streamline that crosses the separatrix once. Let M_- and M_+ be its initial and final points lying at a distance of order 1 from the separatrix. We use $\psi_\pm$, $\varphi_\pm$, $\Phi_\pm$ to denote the values of functions ψ, φ, Φ at the points $M_\pm$. To be specific, we suppose that the point M_- lies in the northern hemisphere ($\psi_- < 0$), and M_+ lies in the southern hemisphere ($\psi_+ > 0$). Suppose also that the streamline segment crosses the separatrix for $\sin\varphi < 0$. It will be shown further, that for $\psi < 0$, the value of ψ grows with every turn of the spiral, as well as the size of the turns. After crossing the separatrix (for $\psi > 0$) the value of ψ grows further, and the size of the turns decreases from one turn to another. The problem is to calculate $\Delta\Phi = \Phi_+ - \Phi_-$ for small ε.

On each turn of the spiral M_- and M_+ mark the point where $\dot{r}= 0, r < \frac{1}{2}$ (the closest to the origin point of the turn). We shall use M_k to represent these points. We enumerate these points so that $k \leq 0$ for $\psi < 0$ and $k > 0$ for $\psi > 0$; increasing $|k|$ corresponds to receding from the separatrix. Thus, M_0 is the last of the points M_k prior to the separatrix crossing, and M_1 is the first of them after the crossing. The turn of the streamline between M_{k-1} and M_k is called the kth turn and denoted by γ_k.

Let ψ_k, φ_k and Φ_k be the values of the functions ψ, φ and Φ in the points M_k. We now evaluate the changes in these functions on the kth turn of the streamline.

For the change in ψ we have:

$$\psi_k - \psi_{k-1} = \int_{\gamma_k} \frac{d\psi}{dt} dt = \int_{\gamma_k} \frac{3}{8}\varepsilon\omega_x \sin\varphi \left(1 - 3\cos^2\theta\right) r^3 \left(r^2 - 1\right) \sin\theta dt. \qquad (16)$$

Using (3) we obtain:

$$\psi_k - \psi_{k-1} = \varepsilon \int_{\gamma_k} \frac{\omega_x}{2} r^2 \sin\varphi \sin\theta dr. \qquad (17)$$

Evidently, the main contribution to this integral is given by the part of γ_k close to the plane $\theta = \frac{\pi}{2}$. We replace γ_k in the integral by $\Gamma_{0,\varphi}$, and, estimating the error introduced as a result, we find:

$$\begin{aligned}\psi_k - \psi_{k-1} &= -\frac{\varepsilon}{6}\omega_x \sin\varphi_k + \varepsilon O\left(\sqrt{|\psi_{k-1}|}\right) + O\left(\varepsilon^2 \ln|\psi_k|\right), \\ &= \varepsilon\Theta_k + \varepsilon O\left(\sqrt{|\psi_{k-1}|}\right) + O\left(\varepsilon^2 \ln|\psi_k|\right).\end{aligned} \tag{18}$$

Here we have introduced the value $\Theta_k = -\frac{\omega_x}{6}\sin\varphi_k$. Analogously, one can see that the main contribution to the change in φ is given by the part of γ_k close to the line $\theta = 0$. For the change in φ we obtain:

$$\varphi_k - \varphi_{k-1} = \varepsilon a(\varphi_{k-1}) \frac{\omega_x \mathrm{sign}(\psi_{k-1})}{\sqrt{|\psi_{k-1}|}} + O(\varepsilon \ln|\psi_k|) + O\left(\varepsilon^2 |\psi_{k-1}|^{-1}\right) \tag{19}$$

where $a(\varphi)$ is defined by (14). The estimates of the residual terms in (18) and (19) were made under the assumption that $C\varepsilon^{3/2} < |\psi_0| < \varepsilon\Theta_0 - C\varepsilon^{3/2}, C = \mathrm{const} > 0$. From (18) and (19) and the expression for the AI (13) we find

$$\Phi_k - \Phi_{k-1} = a_0\omega_x \left[-\frac{\varepsilon\Theta_k \mathrm{sign}(\psi_{k-1})}{\sqrt{|\psi_{k-1}|}} + 2\left(\sqrt{|\psi_k|} - \sqrt{|\psi_{k-1}|}\right)\right] + O\left(\varepsilon^2\left(|\psi_{k-1}|^{-1} + |\psi_k|^{-1}\right)\right). \tag{20}$$

where $a_0 = a(\varphi_0)$. The estimate of the residual term in (20) takes into account that the terms of order ε cancel each other due to the adiabatic invariance of Φ.

The change in the Aadiabatic invariant Φ along a turn well away from the separatrix (at a distance of order 1 from it) is a value of order ε^2. The total change in Φ over such turns is a value of order ε. Consequently, if there is a lower-order term in ε in the asymptotic expression for the total change in Φ, it is due to the turns lying near the separatrix. Therefore, the change $\Delta\Phi$ resulting from the separatrix crossing can be calculated in the leading approximation using (18), (19) and (20), retaining only the leading terms in these expressions. Summing up the changes in Φ along each turn (see (20)), we obtain:

$$\begin{aligned}\Delta\Phi &= a_0\omega_x \sum_{k=-N+1}^{N} \left[-\frac{\varepsilon\Theta_0 \mathrm{sign}(\psi_0 + (k-1)\varepsilon\Theta_0)}{\sqrt{|\psi_0 + (k-1)\varepsilon\Theta_0|}}\right. \\ &+ \left. 2\left(|\psi_0 + k\varepsilon\Theta_0|^{1/2} - |\psi_0 + (k-1)\varepsilon\Theta_0|^{1/2}\right)\right] + O(\varepsilon|\ln\varepsilon|) \\ &+ O\left(\varepsilon^2\left(|\psi_0|^{-1} + |\psi_1|^{-1}\right)\right)\end{aligned} \tag{21}$$

where N is an integer of order $1/\varepsilon$. The leading term in the asymptotic expression does not depend on the exact choice of N. The sum of the terms in parentheses is $O(\varepsilon)$, since all these terms, except for the two extreme ones, cancel out.

We now introduce dimensionless variable $\xi = -\psi_0/\varepsilon\Theta_0$; obviously, $\xi \in (0;1)$. For $\Delta\Phi$, we have:

$$\begin{aligned}\Delta\Phi &= -a_0\omega_x\sqrt{\varepsilon}\Theta_0^{1/2}\sum_{k=-N}^{N-1}\frac{\operatorname{sign}(-\xi+k)}{\sqrt{|-\xi+k|}} + O(\varepsilon|\ln\varepsilon|) + \varepsilon O\left(\xi^{-1}+(1-\xi)^{-1}\right) \\ &= -a_0\omega_x\sqrt{\varepsilon}\Theta_0^{1/2}\sum_{k=0}^{N-1}\left(\frac{1}{\sqrt{-\xi+1+k}}-\frac{1}{\sqrt{\xi+k}}\right) + O(\varepsilon|\ln\varepsilon|) + \varepsilon O\left(\xi^{-1}+(1-\xi)^{-1}\right).\end{aligned} \tag{22}$$

The sum in (22) can be expressed in the form of an integral. Indeed, by definition of the gamma function,

$$\Gamma\left(\frac{1}{2}\right) = p^{1/2}\int_0^\infty t^{-1/2}e^{-pt}dt, p>0.$$

Therefore,

$$\sum_{k=0}^{N-1}\frac{1}{\sqrt{\xi+k}} = \frac{1}{\Gamma(1/2)}\sum_{k=0}^{N-1}\int_0^\infty t^{-1/2}e^{-(\xi+k)t}dt = \frac{1}{\sqrt{\pi}}\int_0^\infty \frac{t^{-1/2}e^{-\xi t}}{1-e^{-t}}\left(1-e^{-Nt}\right)dt.$$

Substituting this expression into (22), we find

$$\begin{aligned}\Delta\Phi &= a_0\omega_x\sqrt{\varepsilon}\Theta_0^{1/2}\frac{1}{\sqrt{\pi}}\int_0^\infty \frac{t^{-1/2}\left(e^{-\xi t}-e^{-(1-\xi)t}\right)}{1-e^{-t}}\left(1-e^{-Nt}\right)dt \\ &+ O(\varepsilon|\ln\varepsilon|) + \varepsilon O\left(\xi^{-1}+(1-\xi)^{-1}\right).\end{aligned}$$

Passing to the limit as $N\to\infty$, we finally obtain:

$$\Delta\Phi = a_0\omega_x\sqrt{\varepsilon}\,|\Theta_0|^{1/2}\frac{1}{\sqrt{\pi}}\int_0^\infty \frac{t^{-1/2}\left(e^{-\xi t}-e^{-(1-\xi)t}\right)}{1-e^{-t}}dt + O(\varepsilon|\ln\varepsilon|) + \varepsilon O\left(\xi^{-1}+(1-\xi)^{-1}\right). \tag{23}$$

In terms of parameters β and φ_0, this formula can be written as

$$\Delta\Phi = \sqrt{\varepsilon}\frac{1}{6\pi}\Gamma^2(3/4)\frac{|\sin\varphi_0|^{1/2}}{(1+\beta^2)^{3/4}}\cos\varphi_0\int_0^\infty \frac{t^{-1/2}\left(e^{-\xi t}-e^{-(1-\xi)t}\right)}{1-e^{-t}}dt \tag{24}$$

$$+ \; O(\varepsilon|\ln\varepsilon|) + \varepsilon O\left(\xi^{-1}+(1-\xi)^{-1}\right).$$

The modulus is used in (23) to ensure that this formula also gives the change in the AI due to the separatrix crossings for $\sin\varphi > 0$. The integral in (23) is a function of ξ. Fig. 4 shows a plot of this function. It has singularities of the form $\xi^{-1/2}$ and $(1-\xi)^{-1/2}$ at the points $\xi = 0$ and $\xi = 1$, respectively.

The quantity ξ in (23) characterizes the separatrix crossing along a certain streamline. It is a function of the initial data ψ_- and φ_-. A small change of order ε in ψ_- and φ_- produces in general a large change of order 1 in ξ. Hence, for small ε it is reasonable to treat ξ as a random value. It can be shown (cf. Ref. [5]) that this random value is uniformly distributed on the interval $(0,1)$. Therefore, $\Delta\Phi$ is also a random value, and its distribution is given by (23). From (23) we find that the mean value of $\Delta\Phi$ is 0 in the leading approximation.

The formula for $\Delta\Phi$, given by (24), was checked numerically for various values of parameters ξ, β, φ_0, and ε. The system (3) was integrated numerically with the use of program TraX [13, 14]. In Fig. 5, log-log plots of $\Delta\Phi(\varepsilon)$ are represented for $\varphi_0 = \frac{5\pi}{3}$ and $\beta = 1.3$, $\xi = 0.3$. The straight lines in Fig.5 correspond to theoretical values of $\Delta\Phi(\varepsilon)$ given by (24), and the asterisks show values obtained numerically from (3) for various values of ε.

5 Diffusion of the adiabatic invariant due to multiple separatrix crossings

The averaged system evolves along the lines $\Phi = \text{const}$ and the averaged motion is periodic for almost all initial data (see Fig. 3). The period of the averaged motion is a value of order $1/\varepsilon$. A trajectory of the averaged system that crosses the separatrix, crosses it twice in one period.

The motion in the exact system in variables ψ and φ can be described as follows. Well away from the separatrix, a point $\psi(t)$, $\varphi(t)$ follows (to within $O(\varepsilon)$) the trajectory of the averaged system $\Phi = \text{const}$. Let this trajectory cross the separatrix. As a small neighborhood of the separatrix is traversed, the value of Φ undergoes a quasirandom jump of order $\sqrt{\varepsilon}$. As a result, after the separatrix has been crossed, the point $\psi(t)$,

$\varphi(t)$ follows a different trajectory of the averaged system. Thus, subsequent separatrix crossings produce intermittent dynamics in the system and diffusion of the AI.

Note from (24) that if $\varphi_0 = \frac{\pi}{2}, \frac{3\pi}{2}$, the change in the AI equals zero in the leading approximation. In the averaged system, the points $\psi = 0, \varphi = \frac{\pi}{2}, \frac{3\pi}{2}$ belong to the phase trajectory defined by $\Phi(\psi, \varphi) = 0$. Consequently, in the exact system, in a small vicinity of the surface $\Phi(\psi, \varphi) = 0$ the diffusion of the AI slows down significantly. Numerical simulations show that it takes considerable time for a streamline to cross the border $\Phi(\psi, \varphi) = 0$.

The process of the diffusion of the AI is illustrated by Figs. 6 and 7. In order to represent a long streamline, we used its Poincare sections by the planes $z = \pm 1/\sqrt{5}$. These planes contain the circles $\psi = \pm\frac{3}{5^{5/2}}$ ($r = \sqrt{3/5}, \cos\theta = \pm\sqrt{3}/3$) filled by degenerate elliptic fixed points of the unperturbed system (see Secion 2). Hence, each close streamline of the unperturbed flow crosses one of these planes twice. In Fig. 6, $\varepsilon = 0.05, \beta = 0.8$ and the phase portrait of the averaged system is one of the types shown in Fig. 3a. There exist two areas of regular dynamics surrounding the circles $\psi = \pm\frac{3}{5^{5/2}}$. The initial conditions for the represented streamline are chosen in the chaotic domain, and it never visits these areas. It is clearly seen in Figs. 6a, 6b, where the Poincare sections of a single streamline by the planes $z = \pm 1/\sqrt{5}$ accordingly are shown. In Fig. 6c, the same streamline is represented on the plane of slow variables ψ, φ. Each dot on the plane corresponds to one crossing of one of the planes $z = \pm 1/\sqrt{5}$ taking place at $r > \sqrt{3/5}$. The time of calculation corresponds approximately to 1000 separatrix crossings, and the diffusion of the AI, both as the intermittent character of motion can be clearly seen. However, in spite of the rather long time of calculation, the streamline does not visit the area of the plane above the curve $\Phi(\psi, \varphi) = 0$, even though it covers all the area between this curve and the curve corresponding to the border of the regular motion area in the upper hemisphere.

In Fig. 7, a single streamline is represented in the same way as in Fig. 6 for $\varepsilon = 0.05, \beta = 0.5$. This case corresponds to the type of the phase portrait of the averaged system shown in Fig. 3c. The whole interior of the sphere is a domain of chaotic dynamics. The time of calculation in Figs. 7a, 7b and 7c corresponds approximately to 500 separatrix crossings. Because of the diffusion, the streamline fills the region corresponding to the area below the curve $\Phi(\psi, \varphi) = 0$ on Fig. 7c, but does not cross this border. However, longer calculation shows that the streamline eventually crosses this border and, during the time corresponding to at least another 500 separatrix crossings, evolves in the area above the line $\Phi(\psi, \varphi) = 0$, where the diffusion process continues in a similar way (see Figs. 7d, 7e and 7f).

Note that the remarkable structures in Figs. 6a and 7a represent similar structures on the plane of the slow variables (see Figs. 6c and 7c), and manifest properties of the corresponding phase portraits of the averaged system (see Figs. 3a and 3c).

Let us make some estimates concerning the diffusion process. As in [5], it can be shown that values of ξ for two successive separatrix crossings can be treated as independent random quantities. Hence, changes in Φ due to multiple separatrix crossings can be regarded as steps of a random walk.

For $\beta > \frac{1}{\sqrt{2}}$, there exist regions filled with streamlines that do not cross the separatrix (cf. [4]). Inside these regions, the AI is conserved to within $O(\varepsilon)$ (see [15]), and the motion is quasiperiodic for most of the initial data.

Consider a streamline that crosses the separatrix. For definiteness let its initial conditions lie in the area $\Phi > 0$. The change in Φ after N separatrix crossings is a value of order $\sqrt{N}\varepsilon^{1/2}$. After $N \sim 1/\varepsilon$ crossings, Φ changes by a value of order 1. It takes time $t \sim \varepsilon^{-2}$. In this time period the streamline will pass close to any point of the chaotic domain belonging to the area $\Phi > 0$. It takes a considerably longer time to cross the border $\Phi = 0$. Thus, the time $t \sim \varepsilon^{-2}$ can be called the chaos development time in the system.

6 Conclusion

We have shown that chaotic advection in the confined Stokes flow (3) arises as a result of accumulation of quasirandom jumps in the adiabatic invariant of the system. These jumps occur due to repeated crossings of the separatrix by a streamline. This mechanism of chaotization produces a chaotic domain of large size for arbitrarily small non-zero value of the perturbation ε. At some parameter values, a large region of regular motion is also present. It can be explained on the basis of phase portraits of the averaged system, which have been constructed.

We have derived the basic formula for the value of the change in the AI that results from the separatrix crossing. It turns out that this change is a quasi-random value of order $\sqrt{\varepsilon}$. The typical chaos development time in the system has been also estimated.

The flow considered is representative of a class of incompressible flows that have the following properties. The velocity field of a flow differs by a small perturbation from a velocity field possessing two integrals of motion. Almost all streamlines of this unperturbed flow are closed. A small perturbation that makes some streamlines cross the separatrix of the unperturbed motion gives rise to chaotic advection in a large domain. The first example of such a flow was given in [3]. The methods developed in [5] and the present paper for investigation of the flows introduced in [3] and [4] can be applied to study other flows of this class.

7 Acknowledgments

This work was performed with the financial support of Russian Basic Research Foundation Grant No. 94-01-00512, 97-01-00350, INTAS Grant No. 93-339-ext, and of the U.S. Civilian Research and Development Foundation for the Independent States of the Former Soviet Union (CRDF) Award No. RM1-184. The authors are grateful to Prof. Stephen Wiggins of California Institute of Technology for pointing out the paper [4]. Prof. Hassan Aref of the Department of Theoretical and Applied Mechanics, University of Illinois at Urbana-Champaign transmitted this report to Prof. James W. Phillips to be published as a TAM Report. Prof. Phillips's assistance in editing the document is greatly appreciated.

Appendix: Derivation of formulas (10)

Consider the quantity $\Delta\Phi = \Phi(\psi + \Delta\psi, \varphi) - \Phi(\psi, \varphi)$ for $\psi > 0, \Delta\psi > 0$. We have

$$\Delta\Phi = -\int_{\Delta S} (\mathbf{v}, \mathbf{n})\, d\sigma \tag{25}$$

where ΔS is part of the surface $\varphi = \text{const}$ bounded by the unperturbed streamlines $\Gamma_{\psi,\varphi}$ and $\Gamma_{\psi+\Delta\psi,\varphi}$, $d\sigma$ is an area element on ΔS, and $\mathbf{n}$ is a unit normal on ΔS, chosen as indicated in Section 3. The minus sign in (25) is due to the fact that the area on the surface $\varphi = \text{const}$ that is bounded by the curve $\Gamma_{\psi,\varphi}$ contracts with increasing ψ.

we introduce the tangential vector $d\mathbf{l}$ on the unperturbed streamline $\Gamma_{\psi,\varphi}$:

$$d\mathbf{l} = [\text{grad}\varphi, \text{grad}\psi]\, dt \tag{26}$$

where dt is an element of time for motion along the streamline. Next, we introduce the following vector with its starting point on the curve $\Gamma_{\psi,\varphi}$:

$$\Delta\mathbf{r} = \frac{[\text{grad}\varphi, \xi]\, \Delta\psi}{(\text{grad}\psi, \text{grad}\varphi, \xi)} \tag{27}$$

where ξ is an arbitrary vector that does not lie in the plane containing the vectors $\text{grad}\psi$ and $\text{grad}\varphi$. The vector $\Delta\mathbf{r}$ is orthogonal to $\text{grad}\varphi$ and its end point lies on the curve $\Gamma_{\psi+\Delta\psi,\varphi}$ to within $O(\Delta\psi^2)$ since $(\text{grad}\psi, \Delta\mathbf{r}) = \Delta\psi$. Thus, using (25)-(27), we obtain in the leading approximation in $\Delta\psi$ the following expression:

$$\Delta\Phi = \oint_{\Gamma_{\psi,\varphi}} (\mathbf{v}, [\Delta\mathbf{r}, d\mathbf{l}]) = \oint_{\Gamma_{\psi,\varphi}} (\text{grad}\varphi, \mathbf{v})\, \Delta\psi dt \tag{28}$$

Hence, and from (8), we obtain the second formula in (10) for $\psi > 0$. This formula in the case $\psi < 0$ and the first formula in (10) can be proved similarly.

References

[1] Aref H., Stirring by chaotic advection. J. Fluid Mech., **143**, 1-21, (1984).

[2] Vainshtein S. I. and Zel'dovich Ya. B., Origin of magnetic fields in astrophysics.Sov. Phys. Usp. **15**, 159, (1972).

[3] Bajer K., Moffatt H.K., On a class of steady confined Stokes flows with chaotic streamlines. J. Fluid Mech., **212**, 337-363, (1990).

[4] Stone H.A., Nadim A. and Strogatz S.H., Chaotic streamlines inside drops immersed in steady Stokes flows. J. Fluid Mech., **232**, 629-646, (1991).

[5] Vainshtein D.L, Vasiliev A.A., Neishtadt A.I., Changes in the adiabatic invariant and streamline chaos in confined incompressible Stokes flow. Chaos, **6**, 1, 67-77, (1996).

[6] Vainshtein D.L., Vasiliev A.A., Neishtadt A.I., Adiabatic chaos in a two-dimensional mapping, Chaos, **6**, 4, 514-518, (1996).

[7] Bogolyubov N.N., Mitropolsky Yu.A., Asymptotic Methods in the Theory of Non-linear Oscillations. New York: Gordon and Breach Science Publ. **537** (1961)

[8] Timofeev A.V., On the constancy of an adiabatic invariant when the nature of the motion changes, Sov. Phys. JETP **48**, 656-659, (1978).

[9] Cary J.R., Escande D.F., Tennyson J., Adiabatic invariant change due to separatrix crossing. Phys. Rev. **A34**, 4256-4275, (1986).

[10] Neishtadt A.I., Change of an adiabatic invariant at a separatrix, Sov.J.Plasma Phys., Sov. J. Plasma Phys. **12**, 568-573, (1986).

[11] Nambu Y., Generalized Hamiltonian dynamics, Phys. Rev. **D7**, 2405-2412, (1975).

[12] Arnol'd V.I., Geometrical Methods in the Theory of Ordinary Differential Equations. New York-Heidelberg-Berlin: Springer-Verlag. XI, 334 (1983)

[13] Levitin V.V., TraX: Simulation and analysis of dynamical systems. Exeter Software, Setauket, New York (1989).

[14] Khibnik A.I. Using TraX: A tutorial to accompany TraX, a program for simulation and analysis of dynamical systems Exeter Software, Setauket, New York (1990).

[15] Arnol'd V.I., Small denominators and problems of stability of motion in classical and celestial mechanics, Russ. Math. Surveys, **18**, 85-192, (1963).

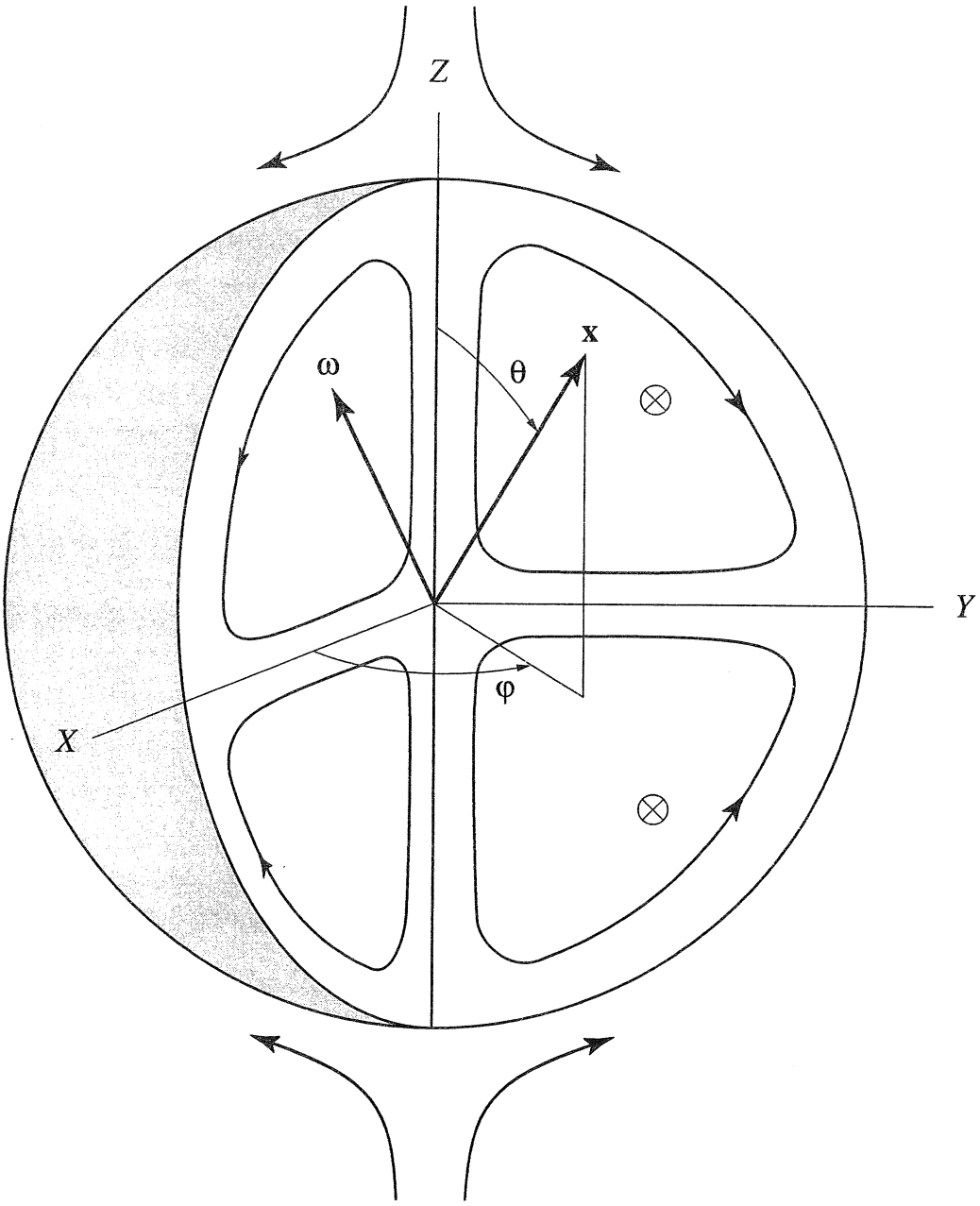

Figure 1: The unperturbed flow.

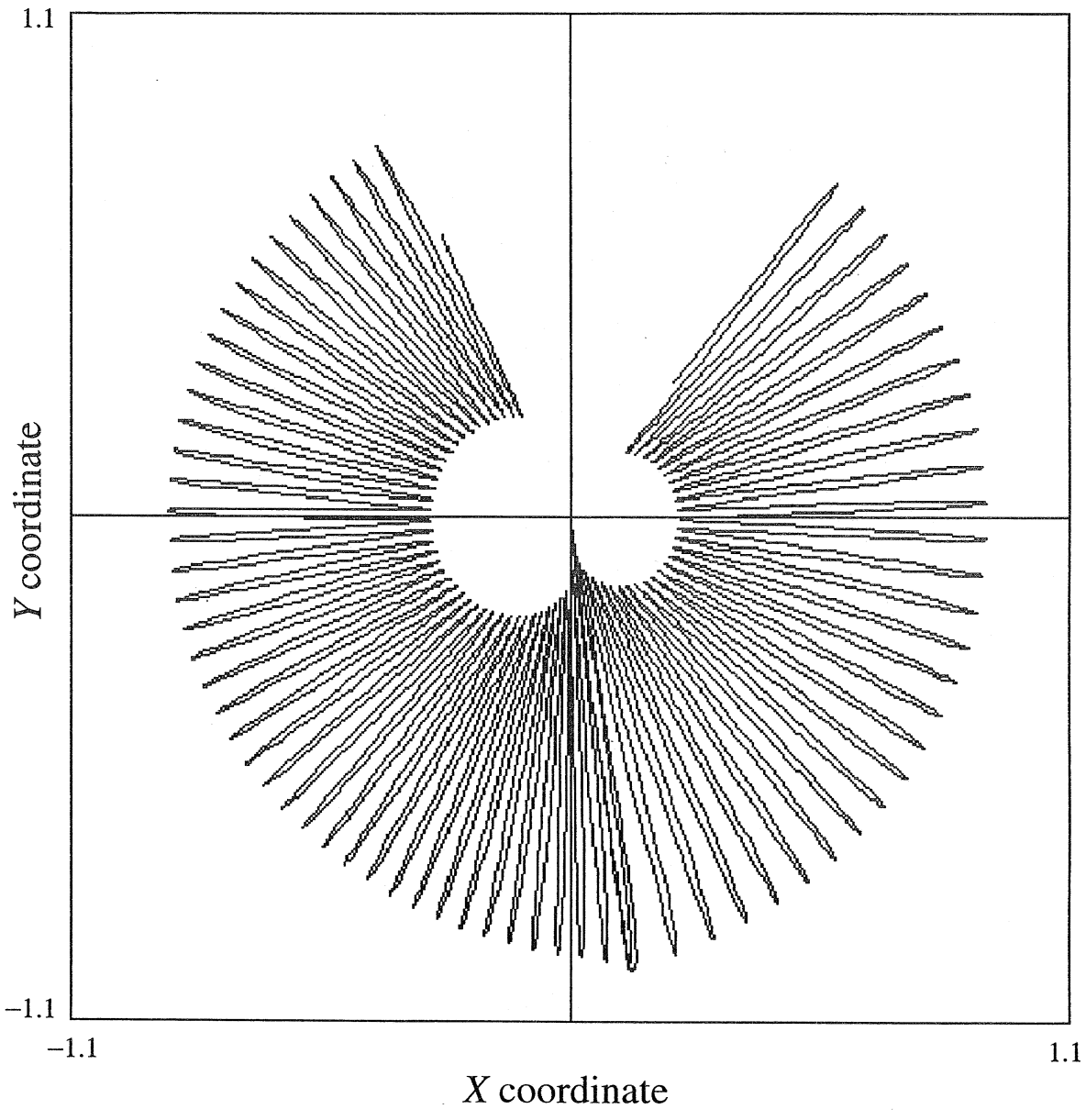

Figure 2: Projections of a streamline segment: (a) on (x, y)-plane.

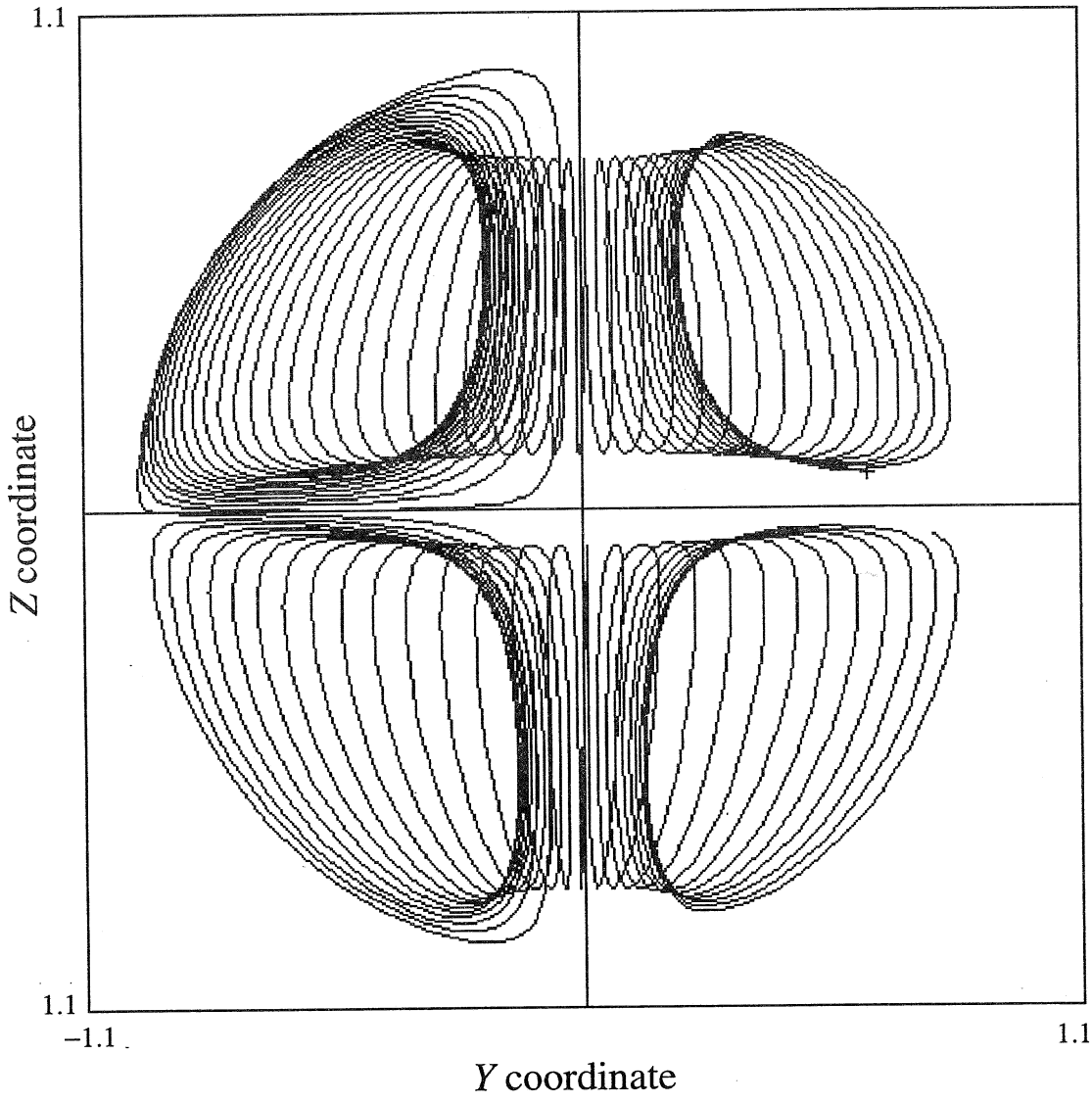

Figure 2 (cont'd): Projections of a streamline segment: (b) on (y, z)-plane.

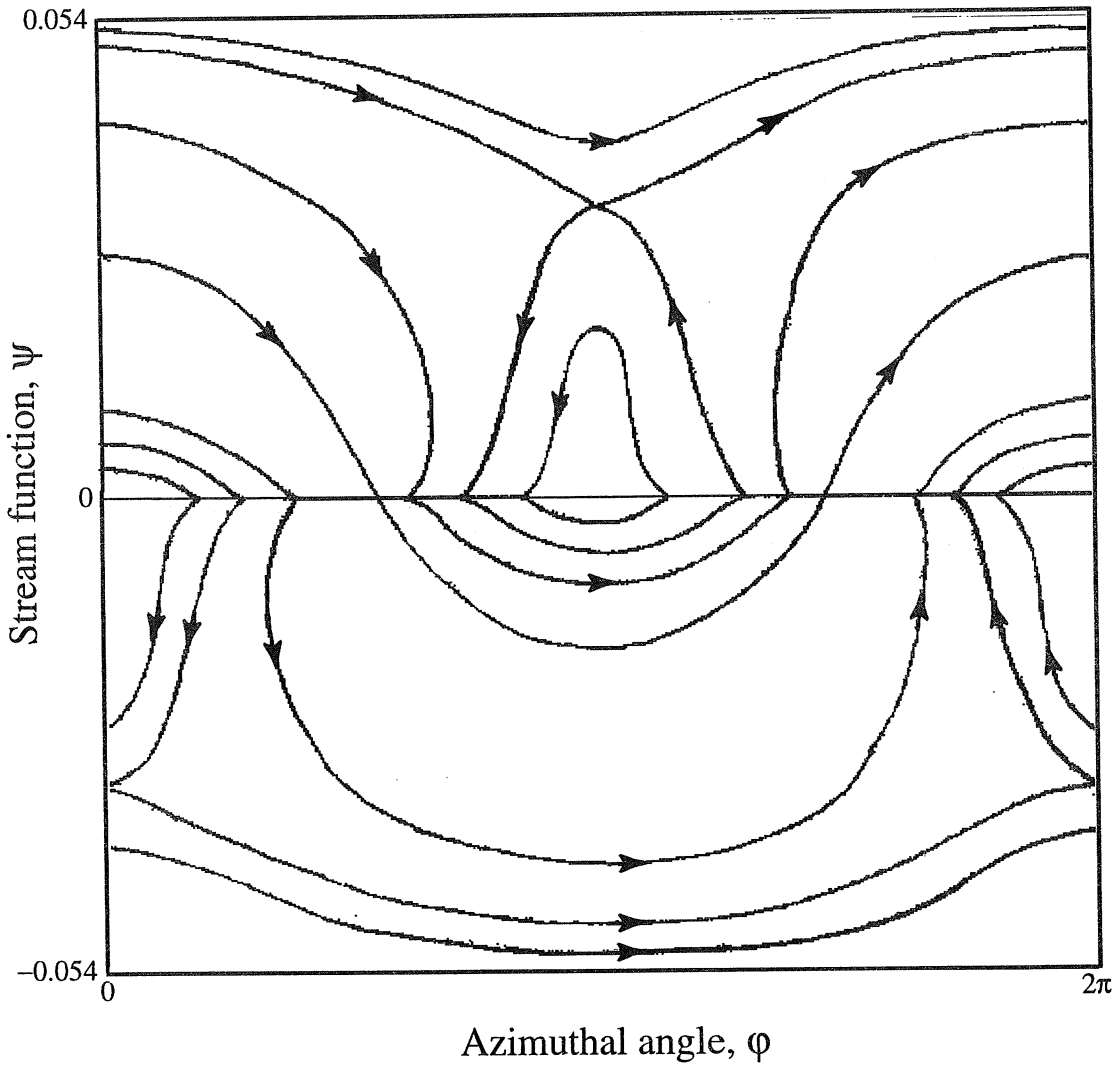

Figure 3: Phase portraits of the averaged system: (a) $\beta > \frac{1}{\sqrt{2}}$.

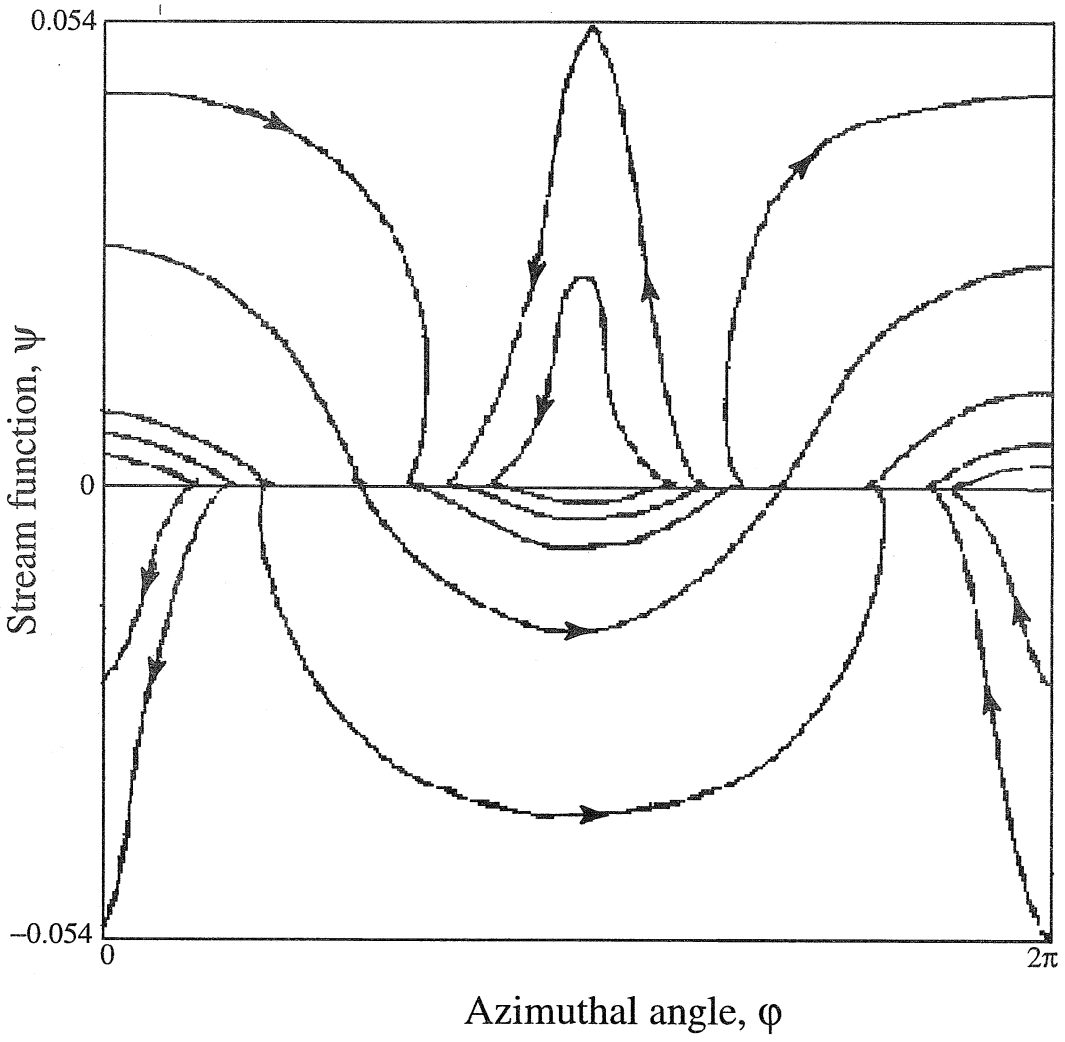

Figure 3 (cont'd): Phase portraits of the averaged system: (b) $\beta = \frac{1}{\sqrt{2}}$.

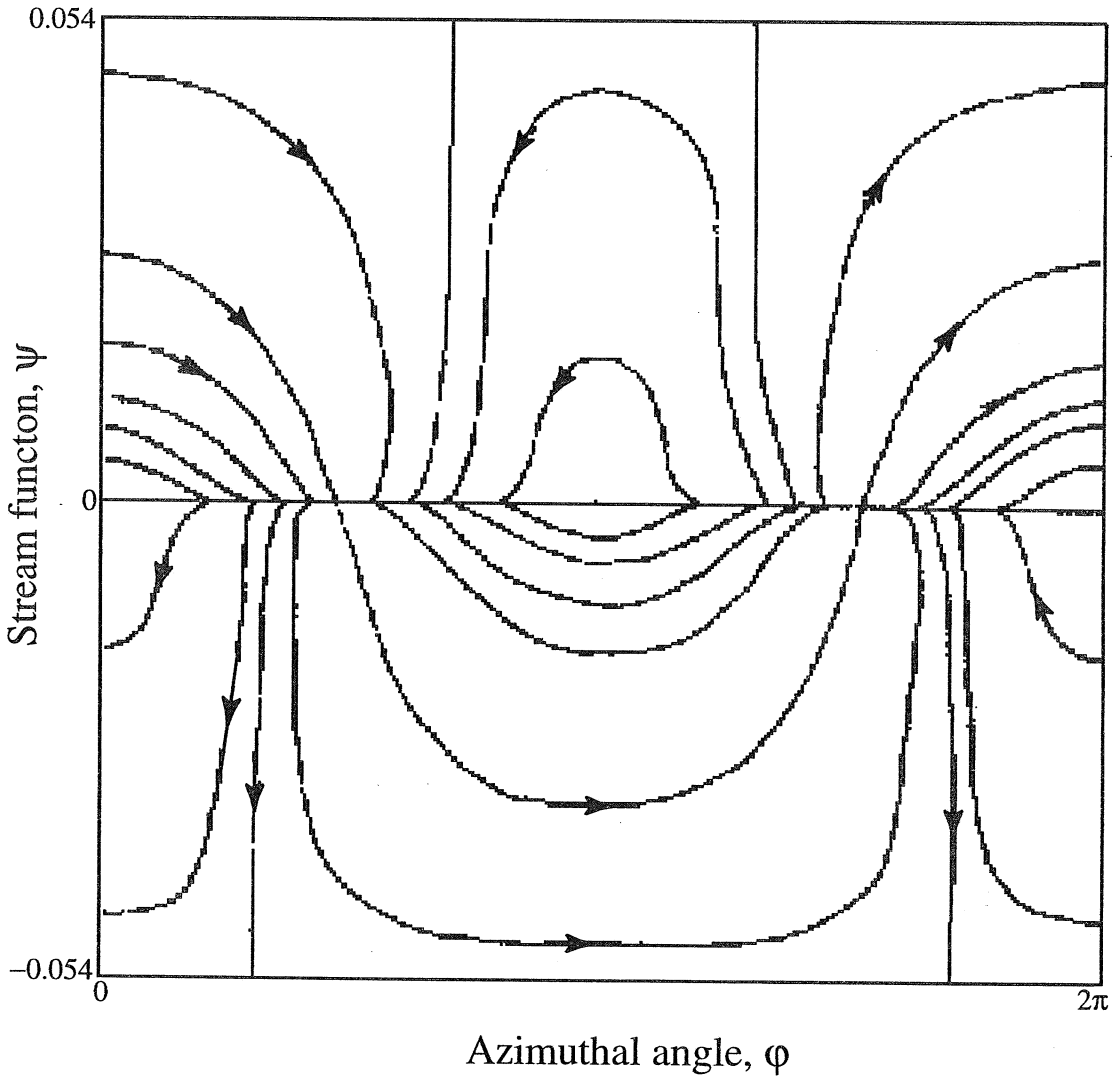

Figure 3 (cont'd): Phase portraits of the averaged system: (c) $\beta < \frac{1}{\sqrt{2}}$.

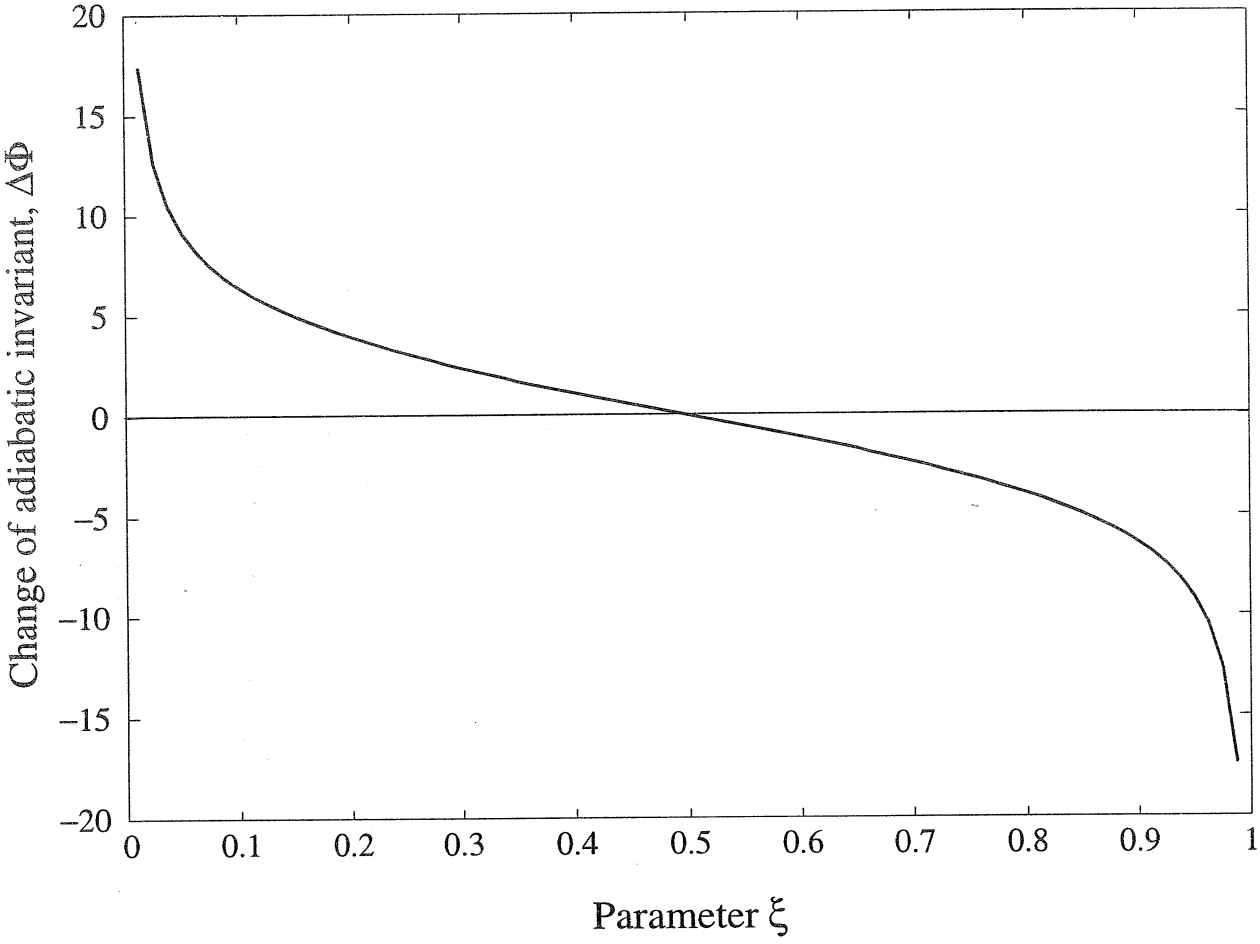

Figure 4: The integral in (23) as a function of ξ.

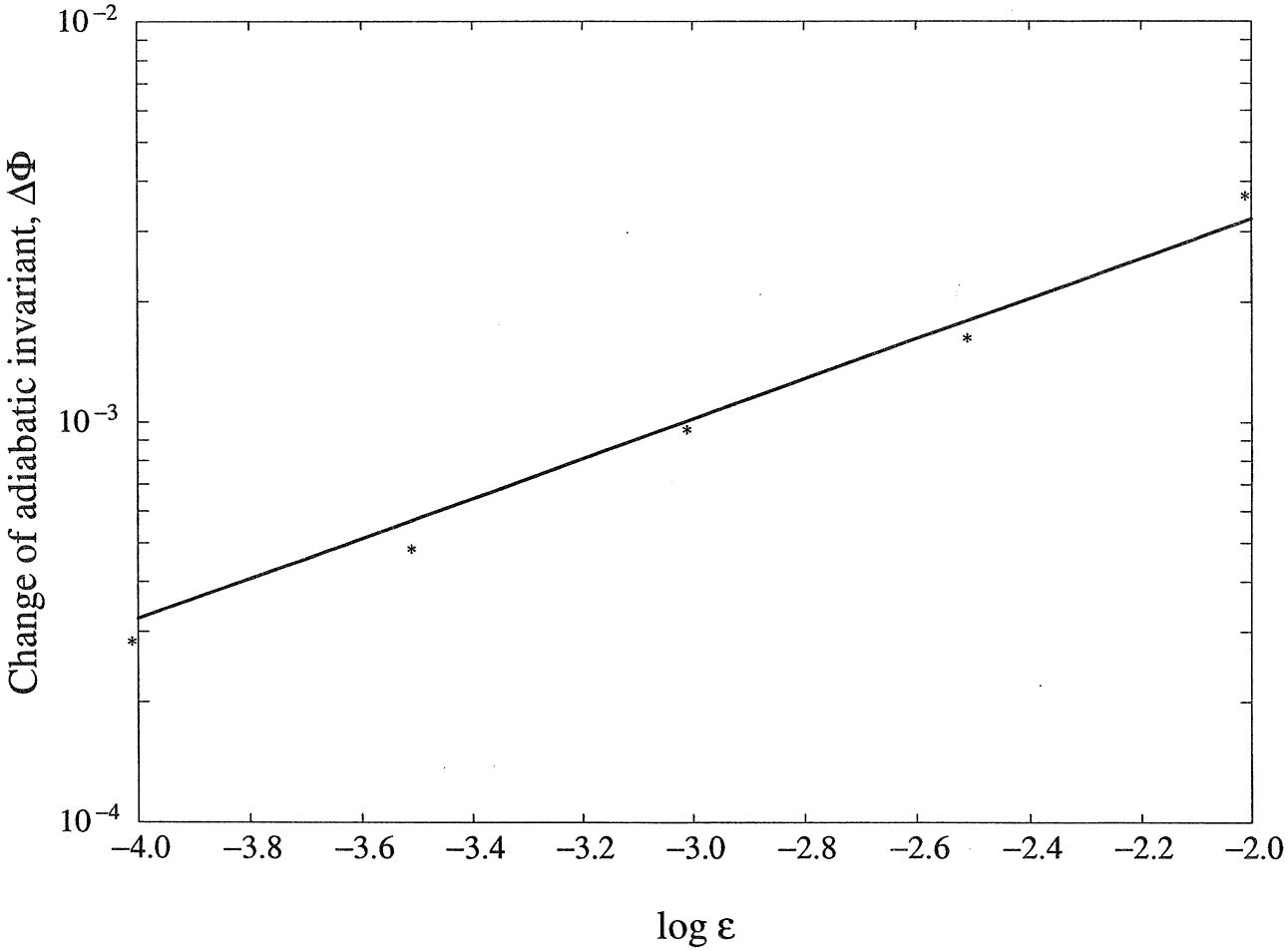

Figure 5: Log-log plots of $\Delta\Phi(\varepsilon)$ for $\varphi_0 = \frac{5\pi}{3}$, $\beta = 1.3$, $\xi = 0.3$. The straight line corresponds to theoretical values given by (24), and the asterisks show values obtained numerically from (3).

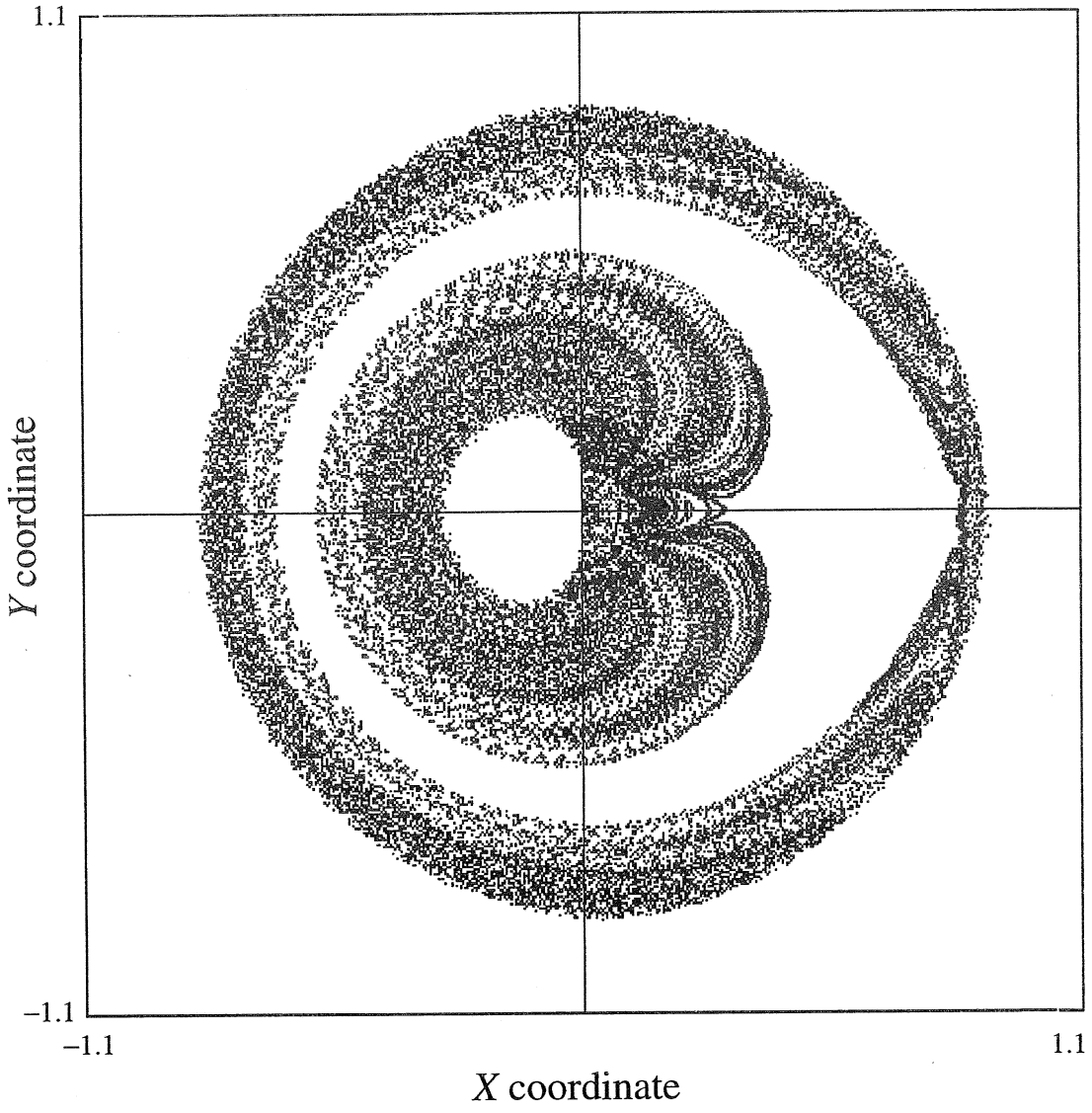

Figure 6: Sections of a long streamline ($\varepsilon = 0.05, \beta = 0.8$, calculation time $t = 200000$) by plane: (a) $z = 1/\sqrt{5}$.

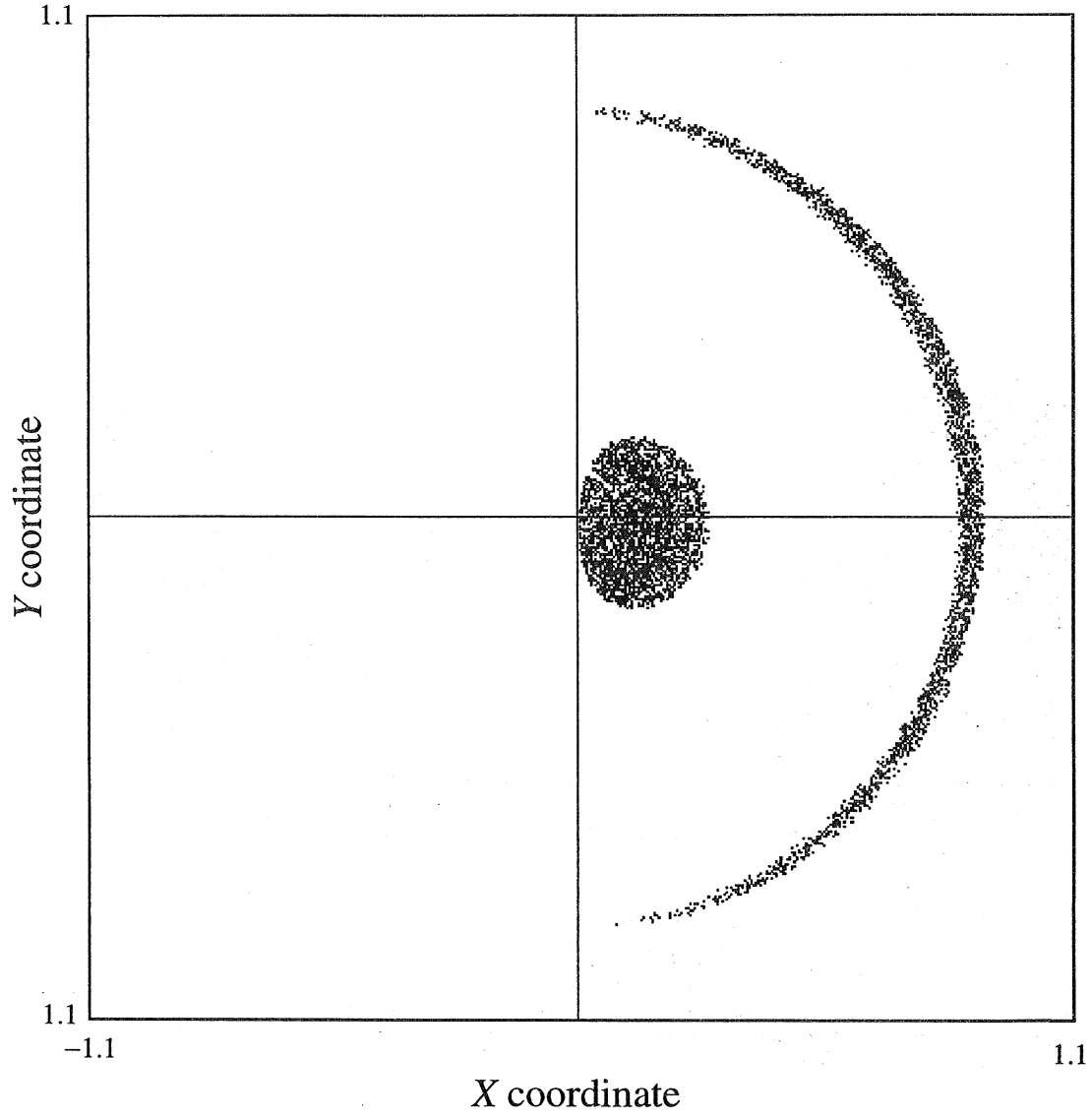

Figure 6 (cont'd): Sections of a long streamline ($\varepsilon = 0.05, \beta = 0.8$, calculation time $t = 200000$) by plane: (b) $z = -1/\sqrt{5}$.

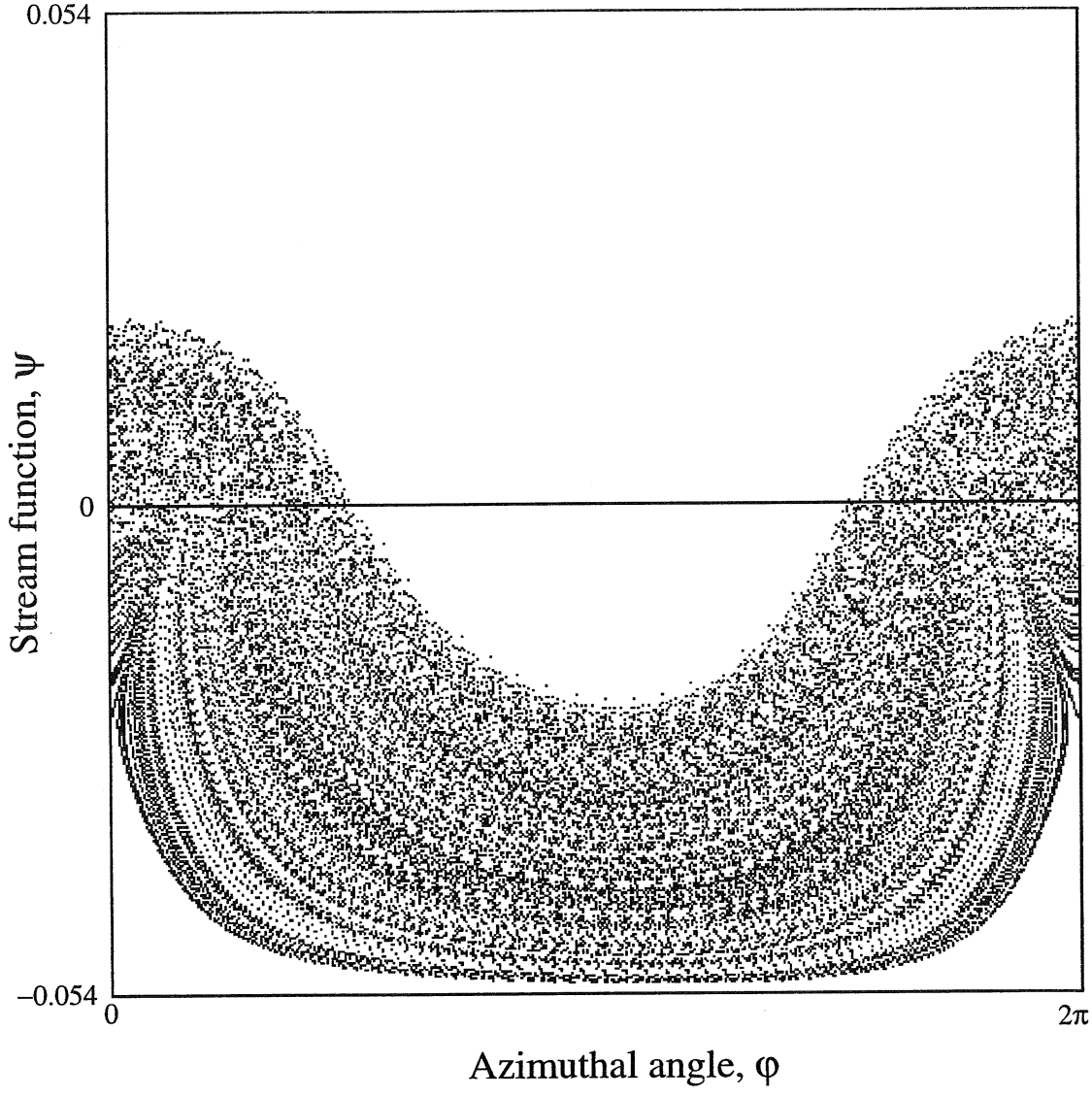

Figure 6 (cont'd): The projection of a long streamline ($\varepsilon = 0.05, \beta = 0.8$, calculation time $t = 200000$) on the (ϕ, ψ)-plane.

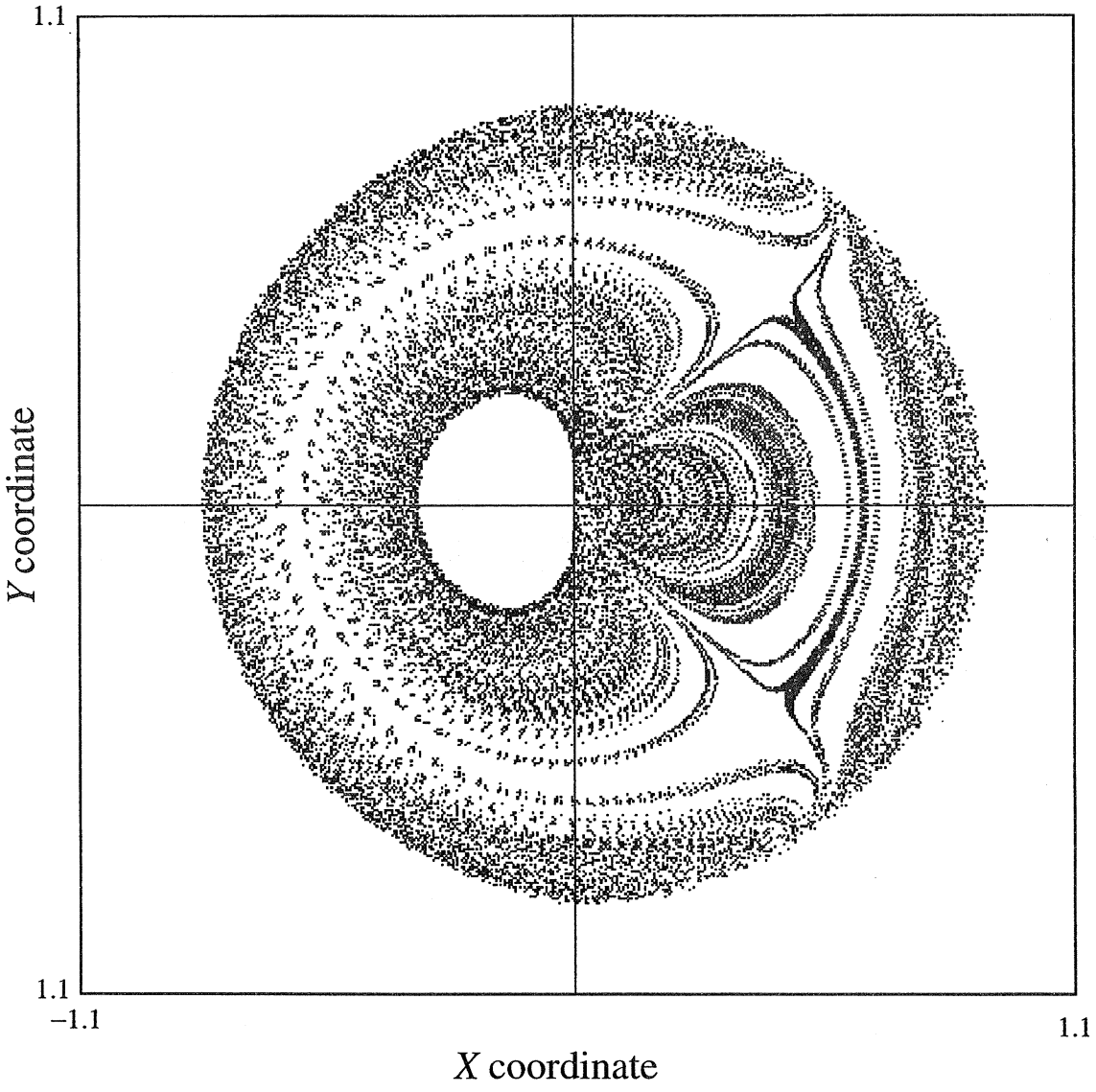

Figure 7: (a). The same as in Fig.5(a), $\varepsilon = 0.05, \beta = 0.5$, calculation time $t = 100000$.

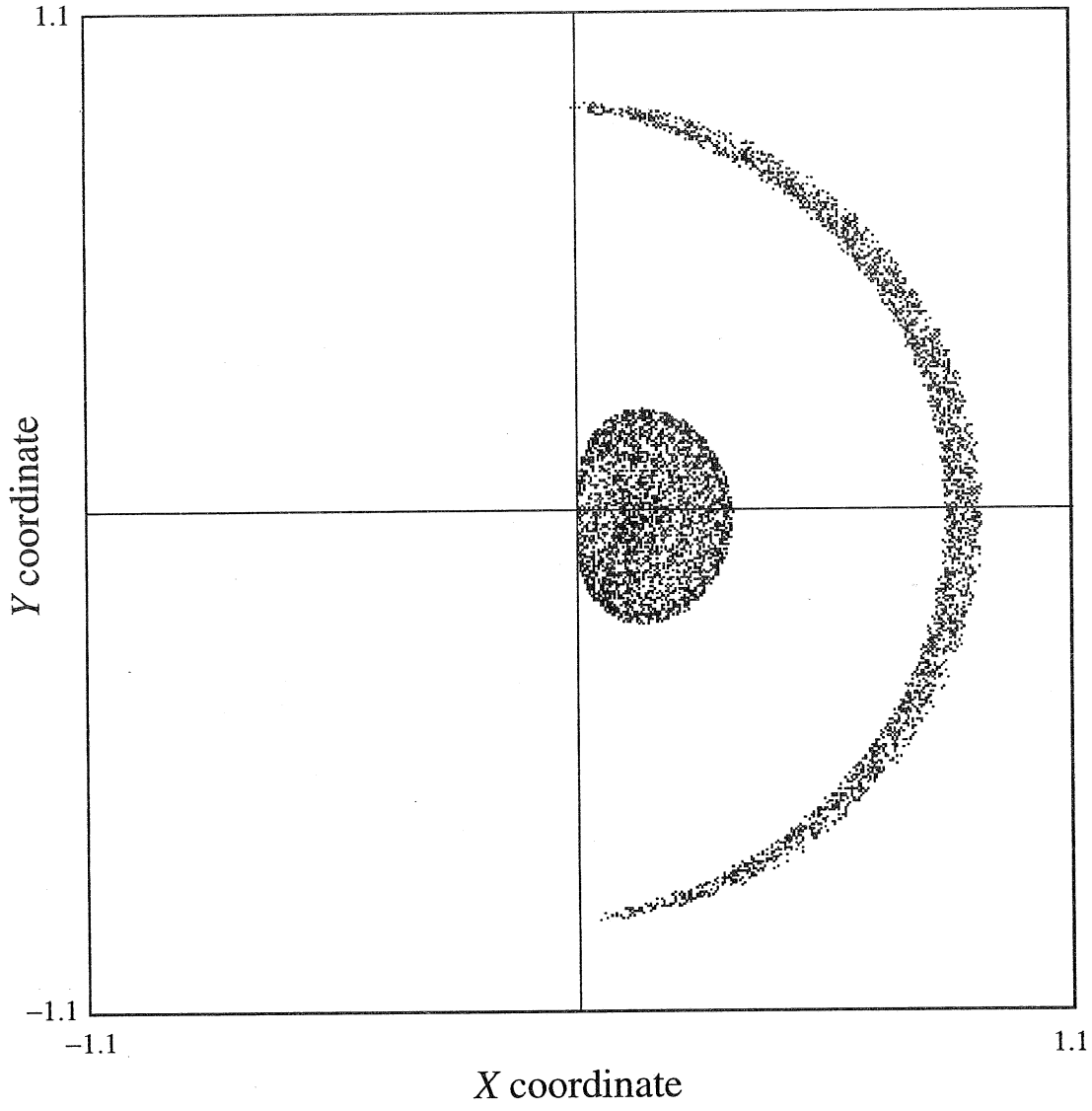

Figure 7 (cont'd): (b). The same as in Fig.5(b), $\varepsilon = 0.05, \beta = 0.5$, calculation time $t = 100000$.

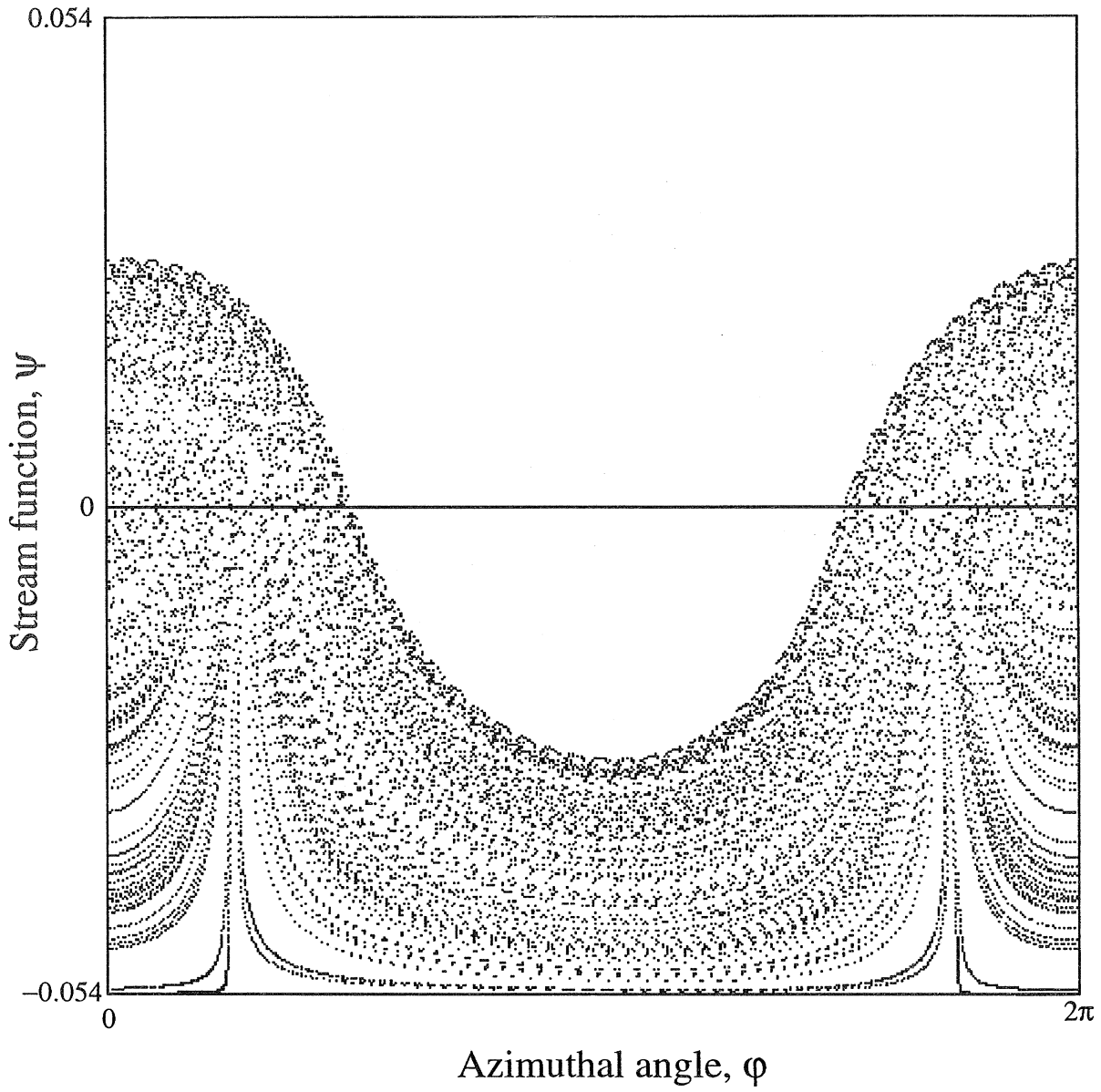

Figure 7 (cont'd): (c). The same as in Fig.5(c), $\varepsilon = 0.05, \beta = 0.5$, calculation time $t = 100000$.

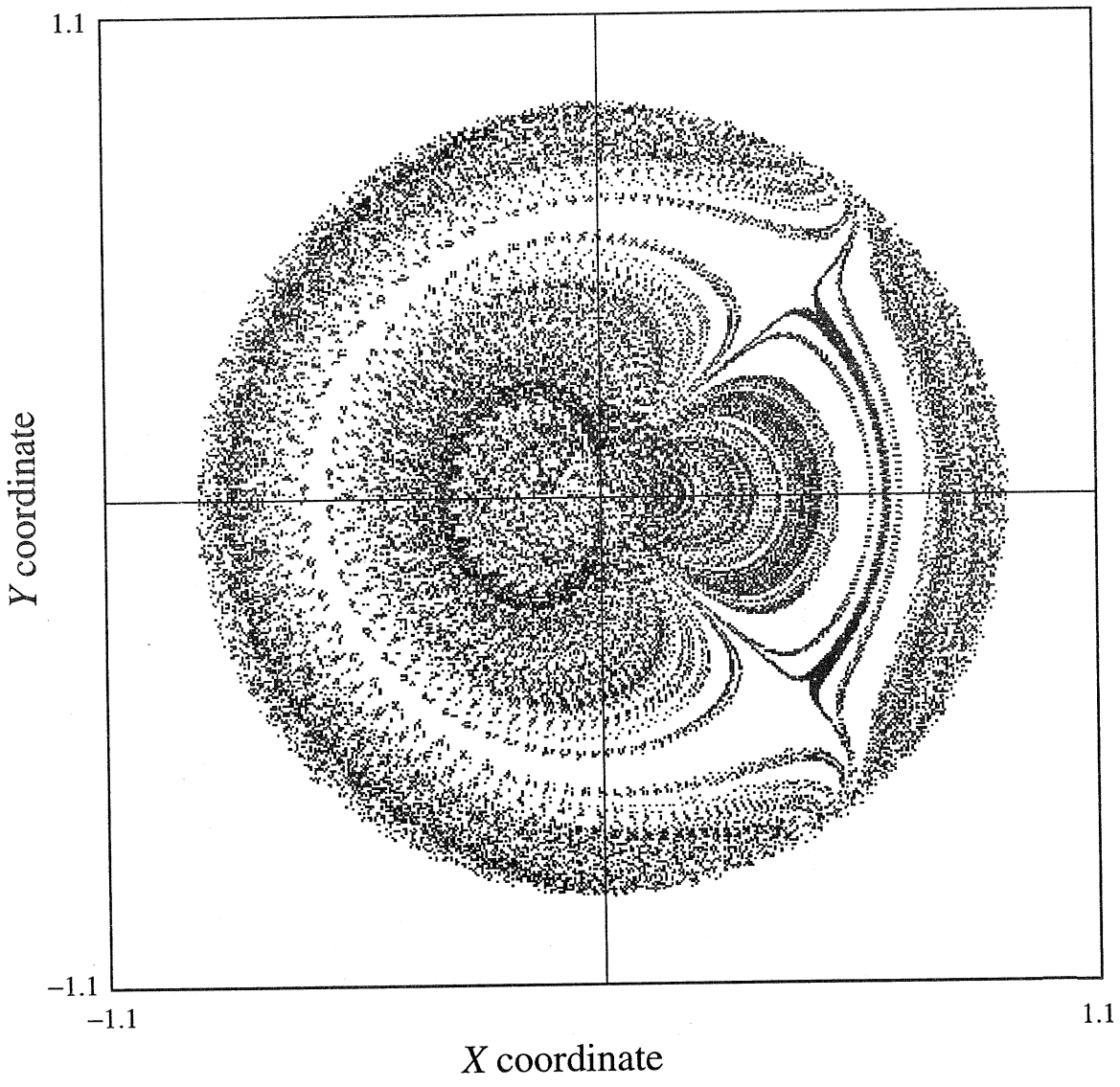

Figure 7 (cont'd): (d). The same as in Fig.7(a), calculation time $t = 200000$.

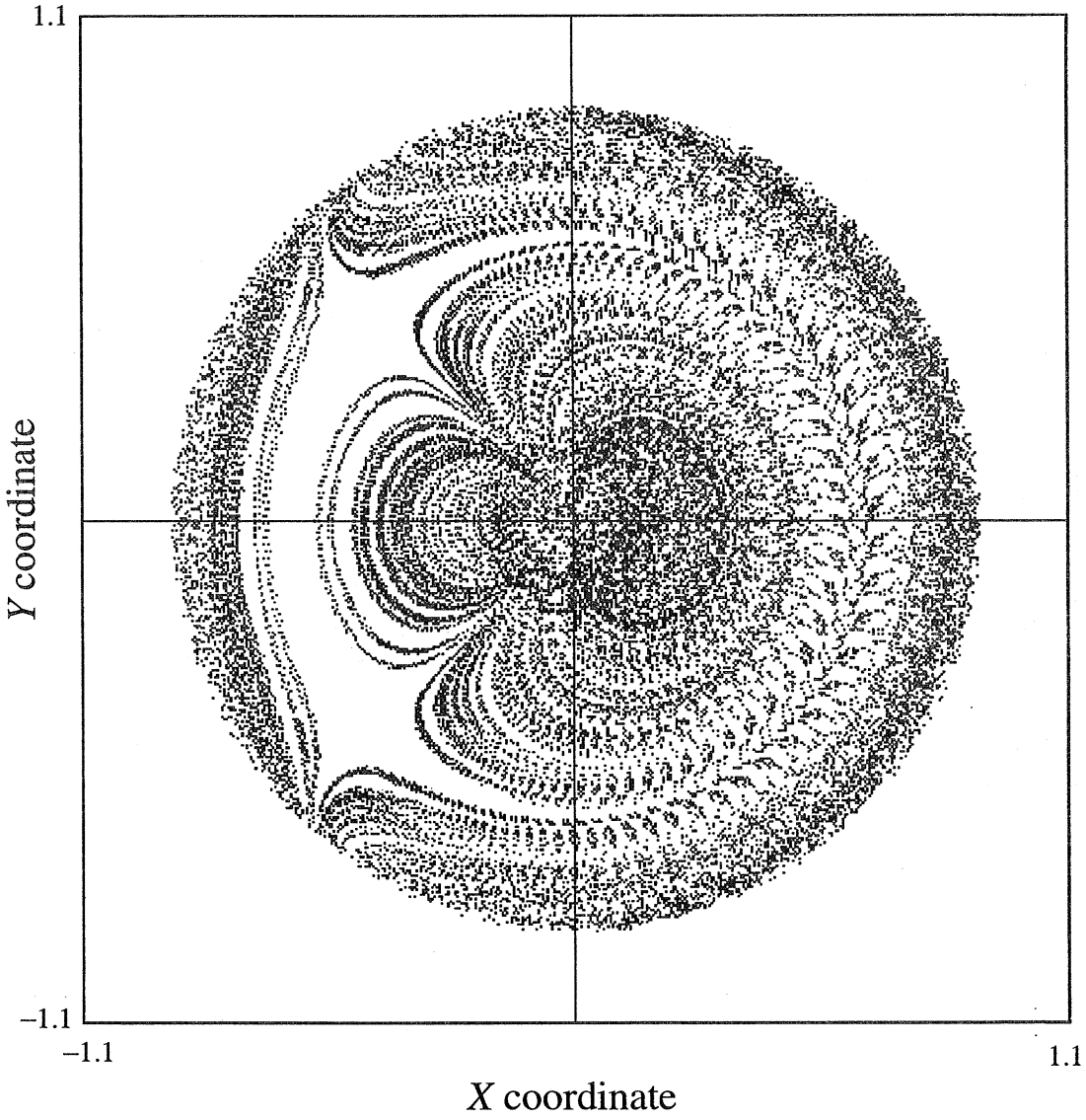

Figure 7 (cont'd): (e). The same as in Fig.7(b), calculation time $t = 200000$.

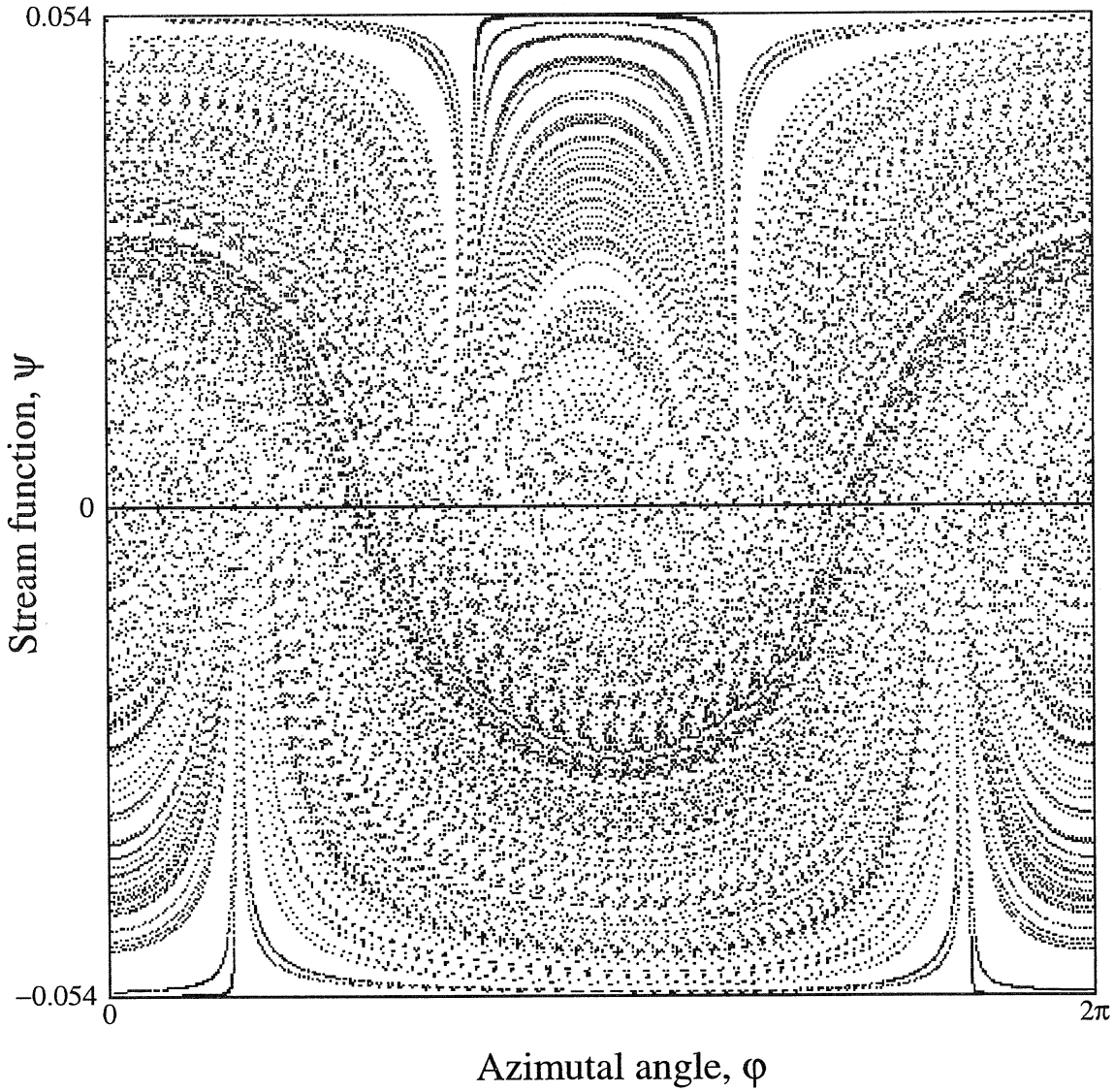

Figure 7 (cont'd): (f). The same as in Fig.7(c), calculation time $t = 200000$.

List of Recent TAM Reports

No.	Authors	Title	Date
771	Lufrano, J. M., and P. Sofronis	Numerical analysis of the interaction of solute hydrogen atoms with the stress field of a crack—*International Journal of Solids and Structures*, 33, 1709–1723 (1996)	Oct. 1994
772	Aref, H., and S. W. Jones	Motion of a solid body through ideal fluid—Proceedings of the DCAMM 25th Anniversary Volume, 55–68 (1994)	Oct. 1994
773	Stewart, D. S., T. D. Aslam, J. Yao, and J. B. Bdzil	Level-set techniques applied to unsteady detonation propagation—In "Modeling in Combustion Science," *Lecture Notes in Physics* , eds. J. Buckmaster and J. Takeno **126**, 390–409 (1996)	Oct. 1994
774	Mittal, R., and S. Balachandar	Effect of three-dimensionality on the lift and drag of circular and elliptic cylinders—*Physics of Fluids* 7, 1841–1865 (1995)	Oct. 1994
775	Stewart, D. S., T. D. Aslam, and J. Yao	On the evolution of cellular detonation	Nov. 1994 *Revised* Jan. 1996
776	Aref, H.	On the equilibrium and stability of a row of point vortices—*Journal of Fluid Mechanics* **290**, 167–181 (1995)	Nov. 1994
777	Cherukuri, H. P., T. G. Shawki, and M. El-Raheb	An accurate finite-difference scheme for elastic wave propagation in a circular disk—*Journal of the Acoustical Society of America*, in press (1996)	Nov. 1994
778	Li, L., and N. R. Sottos	Improving hydrostatic performance of 1–3 piezocomposites—*Journal of Applied Physics* **77**, 4595–4603 (1995)	Dec. 1994
779	Phillips, J. W., D. L. de Camara, M. D. Lockwood, and W. C. C. Grebner	Strength of silicone breast implants—*Plastic and Reconstructive Surgery* **97**, 1215–1225 (1996)	Jan. 1995
780	Xin, Y.-B., K. J. Hsia, and D. A. Lange	Quantitative characterization of the fracture surface of silicon single crystals by confocal microscopy—*Journal of the American Ceramics Society* **78**, 3201–3208 (1995)	Jan. 1995
781	Yao, J., and D. S. Stewart	On the dynamics of multi-dimensional detonation—*Journal of Fluid Mechanics* **309**, 225–275 (1996)	Jan. 1995
782	Riahi, D. N., and T. L. Sayre	Effect of rotation on the structure of a convecting mushy layer—*Acta Mechanica* **118**, 109–120 (1996)	Feb. 1995
783	Batchelor, G. K., and TAM faculty and students	A conversation with Professor George K. Batchelor	Feb. 1995
784	Sayre, T. L., and D. N. Riahi	Effect of rotation on flow instabilities during solidification of a binary alloy—*International Journal of Engineering Science* **34**, 1631–1645 (1996)	Feb. 1995
785	Xin, Y.-B., and K. J. Hsia	A technique to generate straight surface cracks for studying the dislocation nucleation condition in brittle materials—*Acta Metallurgica et Materialia* **44**, 845–853 (1996)	Mar. 1995
786	Riahi, D. N.	Finite bandwidth, long wavelength convection with boundary imperfections: Near-resonant wavelength excitation—*International Journal of Mathematics and Mathematical Sciences*, in press (1996)	Mar. 1995
787	Turner, J. A., and R. L. Weaver	Average response of an infinite plate on a random foundation—*Journal of the Acoustical Society of America* **99**, 2167–2175 (1996)	Mar. 1995
788	Weaver, R. L., and D. Sornette	The range of spectral correlations in pseudointegrable systems: GOE statistics in a rectangular membrane with a point scatterer—*Physical Review E* **52**, 341 (1995)	Apr. 1995
789	Students in TAM 293–294	Thirty-second student symposium on engineering mechanics, J. W. Phillips, coordinator: Selected senior projects by K. F. Anderson, M. B. Bishop, B. C. Case, S. R. McFarlin, J. M. Nowakowski, D. W. Peterson, C. V. Robertson, and C. E. Tsoukatos	Apr. 1995
790	Figa, J., and C. J. Lawrence	Linear stability analysis of a gravity-driven Newtonian coating flow on a planar incline	May 1995

List of Recent TAM Reports (cont'd)

No.	Authors	Title	Date
791	Figa, J., and C. J. Lawrence	Linear stability analysis of a gravity-driven viscosity-stratified Newtonian coating flow on a planar incline	May 1995
792	Cherukuri, H. P., and T. G. Shawki	On shear band nucleation and the finite propagation speed of thermal disturbances—*International Journal of Solids and Structures*, in press (1996)	May 1995
793	Harris, J. G.	Modeling scanned acoustic imaging of defects at solid interfaces—Chapter in *IMA Workshop on Inverse Problems in Wave Propagation*, eds. G. Chevant, G. Papanicolaou, P. Sacks and W. E. Symes, 237–258, Springer-Verlag, New York (1996)	May 1995
794	Sottos, N. R., J. M. Ockers, and M. J. Swindeman	Thermoelastic properties of plain weave composites for multilayer circuit board applications	May 1995
795	Aref, H., and M. A. Stremler	On the motion of three point vortices in a periodic strip—*Journal of Fluid Mechanics* **314**, 1–25 (1996)	June 1995
796	Barenblatt, G. I., and N. Goldenfeld	Does fully-developed turbulence exist? Reynolds number independence versus asymptotic covariance—*Physics of Fluids* **7**, 3078–3082 (1995)	June 1995
797	Aslam, T. D., J. B. Bdzil, and D. S. Stewart	Level set methods applied to modeling detonation shock dynamics—*Journal of Computational Physics*, **126**, 390–409 (1996)	June 1995
798	Nimmagadda, P. B. R., and P. Sofronis	The effect of interface slip and diffusion on the creep strength of fiber and particulate composite materials—Proceedings of the ASME Applied Mechanics Division **213**, 125–143 (1995)	July 1995
799	Hsia, K. J., T.-L. Zhang, and D. F. Socie	Effect of crack surface morphology on the fracture behavior under mixed mode loading—*ASTM Special Technical Publication* 1296, in press (1996)	July 1995
800	Adrian, R. J.	Stochastic estimation of the structure of turbulent fields—*Eddy Structure Identification*, ed. J. P. Bonnet, Springer: Berlin 145–196 (1996)	Aug. 1995
801	Riahi, D. N.	Perturbation analysis and modeling for stratified turbulence	Aug. 1995
802	Thoroddsen, S. T.	Conditional sampling of dissipation in high Reynolds number turbulence—*Physics of Fluids* **8**, 1333–1335	Aug. 1995
803	Riahi, D. N.	On the structure of an unsteady convecting mushy layer—*Acta Mechanica*, in press (1996)	Aug. 1995
804	Meleshko, V. V.	Equilibrium of an elastic rectangle: The Mathieu–Inglis–Pickett solution revisited—*Journal of Elasticity* **40**, 207–238 (1995)	Aug. 1995
805	Jonnalagadda, K., G. E. Kline, and N. R. Sottos	Local displacements and load transfer in shape memory alloy composites	Aug. 1995
806	Nimmagadda, P. B. R., and P. Sofronis	On the calculation of the matrix–reinforcement interface diffusion coefficient in composite materials at high temperatures—*Acta Metallurgica et Materialia*, **44**, 2711–2716 (1996)	Aug. 1995
807	Carlson, D. E., and D. A. Tortorelli	On hyperelasticity with internal constraints—*Journal of Elasticity* **42**, 91–98 (1966)	Aug. 1995
808	Sayre, T. L., and D. N. Riahi	Oscillatory instabilities of the liquid and mushy layers during solidification of alloys under rotational constraint—*Acta Mechanica*, in press (1996)	Sept. 1995
809	Xin, Y.-B., and K. J. Hsia	Simulation of the brittle–ductile transition in silicon single crystals using dislocation mechanics	Oct. 1995
810	Ulysse, P., and R. E. Johnson	A plane-strain upper-bound analysis of unsymmetrical single-hole and multi-hole extrusion processes	Oct. 1995
811	Fried, E.	Continua described by a microstructural field—*Zeitschrift für angewandte Mathematik und Physik*, **47**, 168–175 (1996)	Nov. 1995
812	Mittal, R., and S. Balachandar	Autogeneration of three-dimensional vortical structures in the near wake of a circular cylinder	Nov. 1995

No.	Authors	Title	Date
813	Segev, R., E. Fried, and G. de Botton	Force theory for multiphase bodies—*Journal of Geometry and Physics*, in press (1996)	Dec. 1995
814	Weaver, R. L.	The effect of an undamped finite-degree-of-freedom "fuzzy" substructure: Numerical solutions and theoretical discussion—*Journal of the Acoustical Society of America* **100**, 3159–3164 (1996)	Jan. 1996
815	Haber, R. B., C. S. Jog, and M. P. Bendsøe	A new approach to variable-topology shape design using a constraint on perimeter—*Structural Optimization* **11**, 1–12 (1996)	Feb. 1996
816	Xu, Z.-Q., and K. J. Hsia	A numerical solution of a surface crack under cyclic hydraulic pressure loading	Mar. 1996
817	Adrian, R. J.	Bibliography of particle velocimetry using imaging methods: 1917–1995—*Produced and distributed in cooperation with TSI, Inc., St. Paul, Minn.*	Mar. 1996
818	Fried, E., and G. Grach	An order-parameter based theory as a regularization of a sharp-interface theory for solid–solid phase transitions—*Archive for Rational Mechanics and Analysis*, in press (1996)	Mar. 1996
819	Vonderwell, M. P., and D. N. Riahi	Resonant instability mode triads in the compressible boundary-layer flow over a swept wing—*Physics of Fluids*, in press (1996)	Mar. 1996
820	Short, M., and D. S. Stewart	Low-frequency two-dimensional linear instability of plane detonation—*Journal of Fluid Mechanics*, in press (1997)	Mar. 1996
821	Casagranda, A., and P. Sofronis	On the scaling laws for the consolidation of nanocrystalline powder compacts—Proceedings of the IUTAM Symposium on the Mechanics of Granular and Porous Materials (1996)	Apr. 1996
822	Xu, S., and D. S. Stewart	Deflagration-to-detonation transition in porous energetic materials: A comparative model study—*Journal of Fluid Mechanics*, in press (1997)	Apr. 1996
823	Weaver, R. L.	Mean and mean-square responses of a prototypical master/fuzzy structure—*Journal of the Acoustical Society of America*, in press (1996)	Apr. 1996
824	Fried, E.	Correspondence between a phase-field theory and a sharp-interface theory for crystal growth—*Continuum Mechanics and Thermodynamics*, in press (1997)	Apr. 1996
825	Students in TAM 293–294	Thirty-third student symposium on engineering mechanics, J. W. Phillips, coordinator: Selected senior projects by W. J. Fortino II, A. A. Mordock, and M. R. Sawicki	May 1995
826	Riahi, D. N.	Effects of roughness on nonlinear stationary vortices in rotating disk flows—*Mathematical and Computer Modeling*, in press (1996)	June 1996
827	Riahi, D. N.	Nonlinear instabilities of shear flows over rough walls	June 1996
828	Weaver, R. L.	Multiple scattering theory for a plate with sprung masses: Mean and mean-square responses	July 1996
829	Moser, R. D., M. M. Rogers, and D. W. Ewing	Self-similarity of time-evolving plane wakes	July 1996
830	Lufrano, J. M., and P. Sofronis	Enhanced hydrogen concentrations ahead of rounded notches and cracks—Competition between plastic strain and hydrostatic constraint	July 1996
831	Riahi, D. N.	Effects of surface corrugation on primary instability modes in wall-bounded shear flows	Aug. 1996
832	Bechel, V. T., and N. R. Sottos	Measuring debond length in the fiber pushout test—Proceedings of the ASME Mechanics and Materials Conference (1996)	Aug. 1996
833	Riahi, D. N.	Effect of centrifugal and Coriolis forces on chimney convection during alloy solidification—*Journal of Crystal Growth*, in press (1997)	Sept. 1996
834	Cermelli, P., and E. Fried	The influence of inertia on configurational forces in a deformable solid—*Proceedings of the Royal Society of London A*, in press (1996)	Oct. 1996
835	Riahi, D. N.	On the stability of shear flows with combined temporal and spatial imperfections	Oct. 1996

List of Recent TAM Reports (cont'd)

No.	Authors	Title	Date
836	Carranza, F. L., B. Fang, and R. B. Haber	An adaptive space–time finite element model for oxidation-driven fracture	Nov. 1996
837	Carranza, F. L., B. Fang, and R. B. Haber	A moving cohesive interface model for fracture in creeping materials	Nov. 1996
838	Balachandar, S., R. Mittal, and F. M. Najjar	Properties of the mean wake recirculation region in two-dimensional bluff body wakes	Dec. 1996
839	Ti, B. W., W. D. O'Brien, Jr., and J. G. Harris	Measurements of coupled Rayleigh wave propagation in an elastic plate	Dec. 1996
840	Phillips, W. R. C.	On finite-amplitude rotational waves in viscous shear flows	Jan. 1997
841	Riahi, D. N.	Direct resonance analysis and modeling for a turbulent boundary layer over a corrugated surface	Jan. 1997
842	Liu, Z.-C., R. J. Adrian, C. D. Meinhart, and W. Lai	Structure of a turbulent boundary layer using a stereoscopic, large format video-PIV	Jan. 1997
843	Fang, B., F. L. Carranza, and R. B. Haber	An adaptive discontinuous Galerkin methods for viscoplastic analysis	Jan. 1997
844	Xu, S., T. D. Aslam, and D. S. Stewart	High-resolution numerical simulation of ideal and non-ideal compressible reacting flows with embedded internal boundaries	Jan. 1997
845	Zhou, J., C. D. Meinhart, S. Balachandar, and R. J. Adrian	Formation of coherent hairpin packets in wall turbulence	Feb. 1997
846	Lufrano, J. M., P. Sofronis, and H. K. Birnbaum	Elastoplastically accommodated hydride formation and embrittlement	Feb. 1997
847	Keane, R. D., N. Fujisawa, and R. J. Adrian	Unsteady non-penetrative thermal convection from non-uniform surfaces	Feb. 1997
848	Aref, H., and M. Brøns	On stagnation points and streamline topology in vortex flows	Mar. 1997
849	Asghar, S., T. Hayat, and J. G. Harris	Diffraction by a slit in an infinite porous barrier	Mar. 1997
850	Shawki, T. G., H. Aref, and J. W. Phillips	Mechanics on the Web—Proceedings of the International Conference on Engineering Education (Aug. 1997, Chicago)	Apr. 1997
851	Stewart, D. S., and J. Yao	The normal detonation shock velocity–curvature relationship for materials with non-ideal equation of state and multiple turning points	Apr. 1997
852	Fried, E., A. Q. Shen, and S. T. Thoroddsen	Traveling waves, standing waves, and cellular patterns in a steadily forced granular medium	Apr. 1997
853	Boyland, P. L., H. Aref, and M. A. Stremler	Topological fluid mechanics of stirring	Apr. 1997
854	Parker, S. J., and S. Balachandar	Viscous and inviscid instabilities of flow along a streamwise corner	May 1997
855	Soloff, S. M., R. J. Adrian, and Z.-C. Liu	Distortion compensation for generalized stereoscopic particle image velocimetry	May 1997
856	Zhou, Z., R. J. Adrian, S. Balachandar, and T. M. Kendall	Mechanisms for generating coherent packets of hairpin vortices in near-wall turbulence	June 1997
857	Neishtadt, A. I., D. L. Vainshtein, and A. A. Vasiliev	Chaotic advection in a cubic Stokes flow	June 1997